Research Square

Preprints are preliminary reports that have not undergone peer review.
They should not be considered conclusive, used to inform clinical practice,
or referenced by the media as validated information.

Engineered CXCR3-A expression enhances the trafficking and efficacy of intracerebroventricularly delivered B7-H3-targeting CAR T cells against diffuse intrinsic pontine glioma

Nicholas Vitanza

nicholas.vitanza@seattlechildrens.org

Seattle Children's https://orcid.org/0000-0002-3966-4985

Edward Song

Seattle Children's Research Institute https://orcid.org/0000-0002-4022-9753

Andrea Timpanaro

Seattle Children's Research Institute

Michael Meechan

Seattle Children's Research Institute https://orcid.org/0000-0003-2710-606X

Leonel Sanchez

Ivy Brain Tumor Center at Barrow Neurological Institute

Lucy Li

Benaroya Research Institute https://orcid.org/0000-0003-4616-736X

Sophie Jamet

Seattle Children's Research Institute

Davina Lau

Seattle Children's Research Institute

Lily Winter

Seattle Children's Research Institute

Matthew Dun

University of Newcastle https://orcid.org/0000-0002-9063-5370

Jessica Foster

Children's Hospital of Philadelphia, Philadelphia, PA, USA https://orcid.org/0000-0002-8001-5960

Myron Evans

Seattle Children's Research Institute

Siobhan Pattwell

Seattle Children’s Research Institute

Vandana Kalia

Seattle Children's Research Institute

Surojit Sarkar
Seattle Children's Research Institute
Michael Jensen
Seattle Children's Therapeutics
Matthew Biery
Seattle Children's Resaerch Institute https://orcid.org/0000-0001-6152-3604

Article

Keywords:

Posted Date: April 1st, 2025

DOI: https://doi.org/10.21203/rs.3.rs-6272325/v1

License: This work is licensed under a Creative Commons Attribution 4.0 International License.
Read Full License

Additional Declarations: Yes there is potential Competing Interest. E.Z.S., J.B.F., M.C.J., and N.A.V. are inventors on issued and pending patents related to CAR T cell therapies. M.C.J. holds equity in and is the Chief Scientific Officer of BrainChild Bio, Inc. M.C.J. holds equity in, is a Board Observer for and serves as a member of the Joint Steering Committee of Umoja Biopharma, Inc. N.A.V. holds equity in and serves as the Scientific Advisory Board Chair for BrainChild Bio, Inc. All other authors declare no competing interests.

Version of Record: A version of this preprint was published at Nature Communications on November 11th, 2025. See the published version at https://doi.org/10.1038/s41467-025-64861-6.

Title:

Engineered CXCR3-A expression enhances the trafficking and efficacy of intracerebroventricularly delivered B7-H3-targeting CAR T cells against diffuse intrinsic pontine glioma

Authors and Affiliations:

Edward Z. Song[1], Andrea Timpanaro[1], Michael Meechan[1], Leonel Elena-Sanchez[1], Lucy Z. Li[2,3,4], Sophie Jamet[1], Davina S. Lau[1], Lily I. Winter[1], Matthew D. Dun[5,6,7], Jessica B. Foster[8,9], Myron K. Evans[1], Siobhan S. Pattwell[1], Vandana Kalia[1], Surojit Sarkar[10], Michael C. Jensen[11], Matthew C. Biery[1], Nicholas A. Vitanza[1,12]

[1]Ben Towne Center for Childhood Cancer and Blood Disorder Research, Seattle Children's Research Institute, Seattle, WA, USA
[2]Center for Fundamental Immunology, Benaroya Research Institute, Seattle, WA, USA
[3]Medical Scientist Training Program, University of Washington, Seattle, WA
[4]Molecular and Cellular Biology Program, University of Washington, Seattle, WA
[5]Cancer Signaling Research Group, School of Biomedical Sciences and Pharmacy, College of Health, Medicine and Wellbeing, University of Newcastle, Callaghan, NSW, Australia
[6]Paediatric Stream, Mark Hughes Foundation Centre for Brain Cancer Research, College of Health, Medicine and Wellbeing, University of Newcastle, Callaghan, NSW, Australia
[7]Precision Medicine Research Program, Hunter Medical Research Institute, New Lambton Heights, NSW, Australia
[8]Department of Pediatrics, University of Pennsylvania Perelman School of Medicine, Philadelphia, PA, USA
[9]Division of Oncology, Children's Hospital of Philadelphia, Philadelphia, PA, USA
[10]Department of Pathology, University of Washington, Seattle, WA, USA
[11]Seattle Children's Therapeutics, Seattle, WA, USA
[12]Department of Pediatrics, Seattle Children's Hospital, University of Washington, Seattle, WA, USA

Running Title:

CXCR3-A-modified B7-H3 CAR T cells against DIPG

Corresponding Author:

Nicholas A. Vitanza, MD
Seattle Children's Hospital, M/S Cure-09, 1920 Terry Avenue Seattle, WA 98101
Ph: 206-884-4084 Fax: 206-884-4100 Email: nicholas.vitanza@seattlechildrens.org

Competing Interests:

E.Z.S., J.B.F., M.C.J., and N.A.V. are inventors on issued and pending patents related to CAR T cell therapies. M.C.J. holds equity in and is the Chief Scientific Officer of BrainChild Bio, Inc. M.C.J. holds equity in, is a Board Observer for and serves as a member of the Joint Steering Committee of Umoja Biopharma, Inc. N.A.V. holds equity in and serves as the Scientific Advisory Board Chair for BrainChild Bio, Inc. All other authors declare no competing interests.

Word Count: 4019 for Introduction + Results + Discussion.
Number of Figures and Tables: 7 figures and no table
Extended Data: 9 figures

Abstract: (148 words)

Diffuse intrinsic pontine glioma (DIPG) is a fatal brainstem tumor desperately in need of better treatments. CAR T cell therapies for DIPG have demonstrated clinical tolerability and bioactivity, but not universal benefit. A major obstacle is insufficient CAR T cell trafficking to the tumor. As our clinical trials have demonstrated locoregional elevation of CXCL10, a ligand of the chemokine receptor CXCR3, we aimed to leverage this CXCL10 to enhance cell trafficking by engineering our B7-H3-targeting CAR T cells to overexpress CXCR3 variants. Here, we demonstrate that, compared to unmodified B7-H3 CAR T cells, CXCR3-A-modified CAR T cells migrate more efficiently toward CXCR3 ligands in vitro, and when delivered intracerebroventricularly in orthotopic DIPG mouse models, CXCR3-A-modified CAR T cells show enhanced trafficking into the tumor and improved therapeutic efficacy. Overall, our data support the potential for engineering CXCR3-A expression to enhance CAR T cell trafficking and efficacy against DIPG.

Introduction:

Central nervous system (CNS) tumors have surpassed leukemia as the leading cause of fatality among children with cancer[1]. Among the pediatric CNS tumors, diffuse intrinsic pontine glioma (DIPG) is particularly devastating, affecting approximately 400 children per year in the US at a median age of 7[2,3]. DIPG is an aggressive and universally fatal brainstem tumor, for which surgical excision is not feasible, and chemotherapy is largely ineffective. Focal radiation is the only standard treatment option, yet it solely provides a palliative benefit, as most patients die within a year. Therefore, more effective treatments against DIPG are desperately needed.

Chimeric antigen receptor (CAR) T cell therapies targeting various antigens have been developed to treat pediatric CNS tumors including DIPG[4]. However, despite evidence of feasibility, tolerability, and some CAR T cell bioactivity in phase 1 clinical trials, the overall efficacy remains limited. Among the challenges[5,6], insufficient CAR T cell trafficking to the tumor has been a major obstacle to successful CAR T cell treatment against solid tumors such as DIPG. Therefore, to address this issue, we engineered our B7-H3-targeting CAR T cells (B7-H3 CAR T cells), which have been clinically studied and well tolerated in our phase 1 trial (CT04185038)[7,8], to overexpress the chemokine receptor CXCR3 to promote CAR T cell trafficking and improve their efficacy against DIPG.

CXCR3 is a chemokine receptor that interacts with the chemokines CXCL10, CXCL9, and CXCL11 and directs cell migration against the concentration gradient of these ligands[9]. Given that CXCL10 is produced by activated T cells[10] and that CXCL10 is upregulated in the cerebrospinal fluid (CSF) of pediatric CNS tumor patients following intracranial CAR T cell treatment[7,8], we hypothesized that the interaction between CXCL10 and CXCR3 could be leveraged to enhance CAR T cell trafficking to the tumor by overexpressing CXCR3 in CAR T cells. In addition, with more CXCR3-modified CAR T cell trafficking to the tumor, more CXCL10 would be produced, further amplifying CAR T cell recruitment through positive feedback. Therefore, this new iteration of CAR T cell technology could be more effective in treating children with DIPG.

Many efforts to promote CAR T cell trafficking to solid tumors have been devoted to capitalizing on the chemokines upregulated by the tumor types of interest. For example, it was shown that glioblastoma cell lines express CXCL8 post-irradiation and CAR T cells engineered to express the receptors for CXCL8 can migrate more effectively to the irradiated tumor in the mouse brain by intravenous (IV) injection[11]. In contrast, our strategy aims to take advantage of the chemokines expressed by antigen-stimulated CAR T cells such as CXCL10, given the clinical evidence of CXCL10 upregulation following CAR T cell doses[7,8,12]. While endogenous CXCR3 is expressed on activated T cells[13], here we investigated whether overexpressing CXCR3 could further sensitize CAR T cells to migrate toward CXCL10.

In this study, we demonstrate that B7-H3 CAR T cells engineered to overexpress the CXCR3 isoform CXCR3-A can migrate more efficiently toward the CXCR3 ligands such as CXCL10 in vitro, in comparison to the standard B7-H3 CAR T cells. In vivo, CXCR3-A-modified CAR T cells show enhanced trafficking to the tumor sites post intracerebroventricular (ICV) delivery and result in

improved efficacy in treating orthotopic DIPG xenograft mouse models. Overall, our data support the potential for engineering CXCR3-A overexpression to enhance CAR T cell trafficking to the tumor and improve the efficacy of CAR T cell therapy for DIPG. To our knowledge, we are the first to investigate the trafficking of chemokine receptor-modified CAR T cells via ICV delivery, which is clinically significant for CNS tumors.

Results:

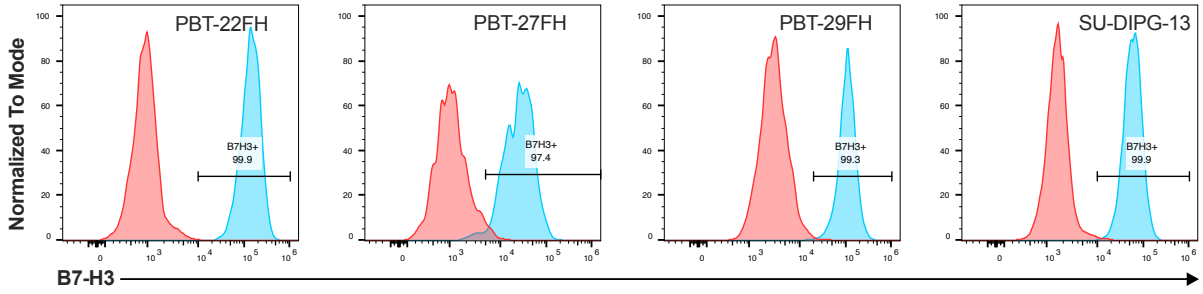
B7-H3 CAR T cells are cytotoxic against patient-derived DIPG cells and able to produce CXCL10

Several CAR T cell therapies with various antigen specificities have been developed[7,8,12,14] and clinically investigated in a series of first-in-human phase 1 trials at Seattle Children's for pediatric CNS tumors using intracranial delivery[15,16]. We focused our study on the B7-H3 CAR T cells, which have demonstrated clinical tolerability after ICV delivery to children with DIPG[7,8]. B7-H3 (CD276) is a member of the B7 family of immunoregulatory proteins and is highly expressed on DIPG tumor cells[17,18], including our treatment-naïve biopsy-derived DIPG cells[19] (PBT-22FH, PBT-27FH, and PBT-29FH) and an autopsy-derived DIPG cell line (SU-DIPG-13) used in this study (Figure 1A). We validated that the B7-H3 CAR T cells could kill the primary DIPG cells when co-cultured in vitro (Figure 1B) and produce CXCL9 and CXCL10 post-stimulation, although CXCL11 was not significantly released (Figure 1C).

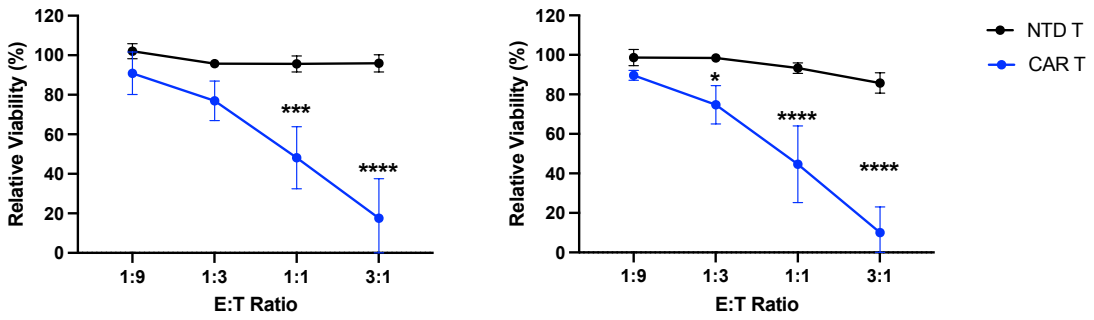
Manufactured CAR T cells heterogeneously express CXCR3 and can migrate toward CXCL10

CXCR3 is upregulated by activated T cells[13], and since T cell activation is the first step to generate CAR T cells among widely used protocols, we expected manufactured CAR T cells to display some endogenous expression of CXCR3. To confirm this, we isolated T cells from healthy donors' peripheral blood mononuclear cells (PBMC), activated them with clinically used anti-CD3/CD28 beads, and generated CAR T cells, which did result in a heterogeneous increase of CXCR3 surface expression (Figure 1D). To test CAR T cell migration efficiency in vitro for this study, we first used our standard B7-H3 CAR T cells to establish a trans-well chemotaxis assay. CAR T cells were seeded in the insert wells that allow them to migrate through a membrane with 5-μm pores into the bottom wells with chemoattractant, and the number of CAR T cells in the bottom wells were counted and normalized to the seeded cell number. As the CAR T cells had endogenous CXCR3 expression, they were able to migrate toward CXCL10 in a dose-dependent manner within 2 hours (Figure 1E). We further established a trans-well killing assay, in which CAR T cells were permitted to migrate for 2 hours then co-cultured overnight with DIPG cells seeded in the bottom wells. As CXCL10 could induce CAR T cell migration, significantly more DIPG cells were killed when seeded with CXCL10 (Figure 1F). Given that CXCL10 neither directly inhibited DIPG tumor viability (Figure 1G) nor affected CAR T cell cytotoxicity against DIPG cells (Figure 1H) in the control experiments, the reduced tumor viability in the cultures with CXCL10 in Figure 1F reflects CXCL10-induced CAR T cell migration.

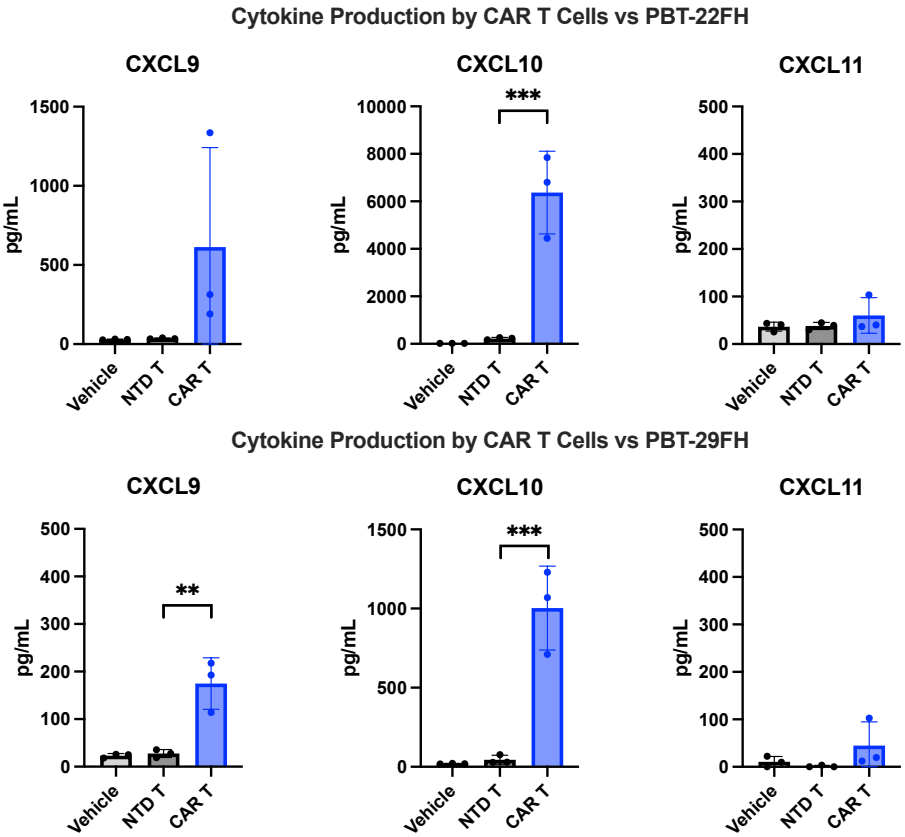
1A


PBT-22FH
PBT-27FH
PBT-29FH
SU-DIPG-13
Normalized To Mode
B7H3+
99.9
97.4
99.3
B7-H3

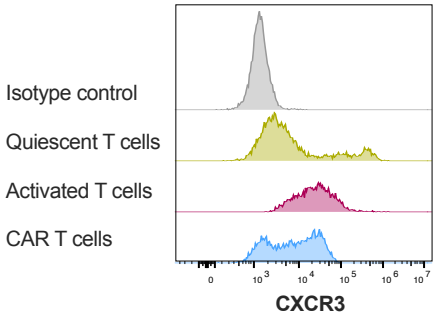
1B


CAR T Cell Direct Killing PBT-22FH (24h)
CAR T Cell Direct Killing PBT-29FH (24h)
Relative Viability (%)
E:T Ratio
1:9
1:3
1:1
3:1
NTD T
CAR T
***
****
*

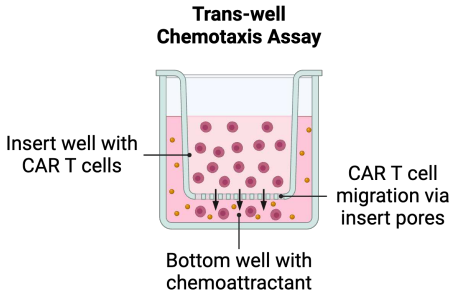
1C

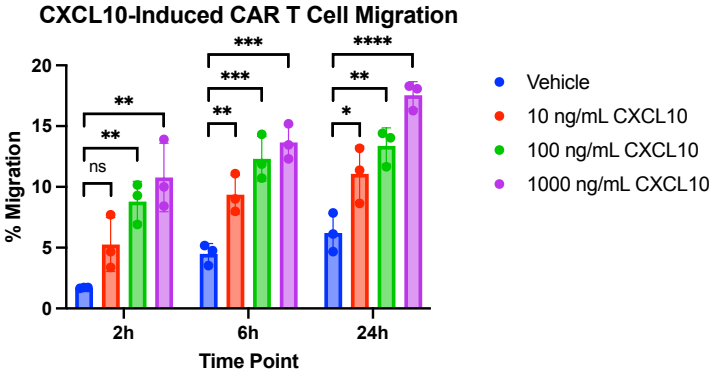

Cytokine Production by CAR T Cells vs PBT-22FH
Cytokine Production by CAR T Cells vs PBT-29FH
CXCL9
CXCL10
CXCL11
pg/mL
Vehicle
NTD T
CAR T
**
***

1D

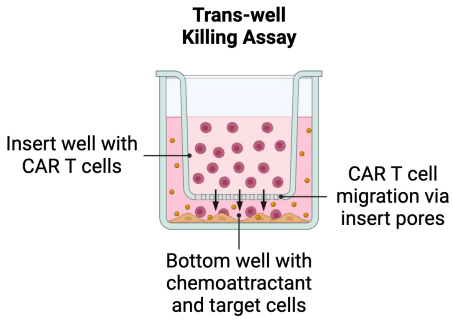


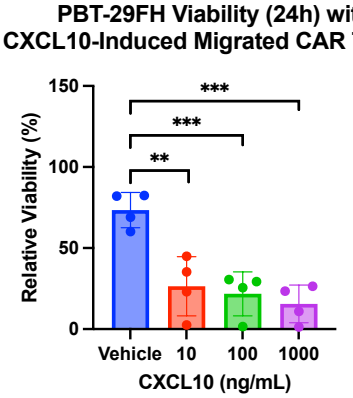
1E



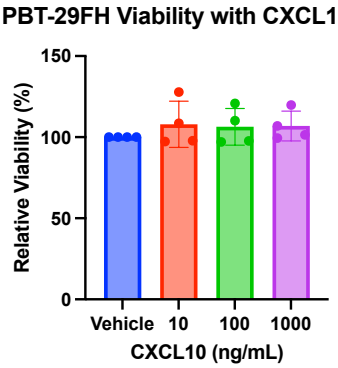


1F

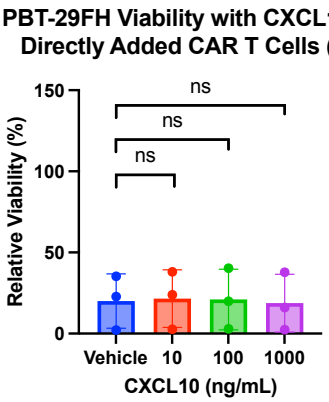




1G



1H



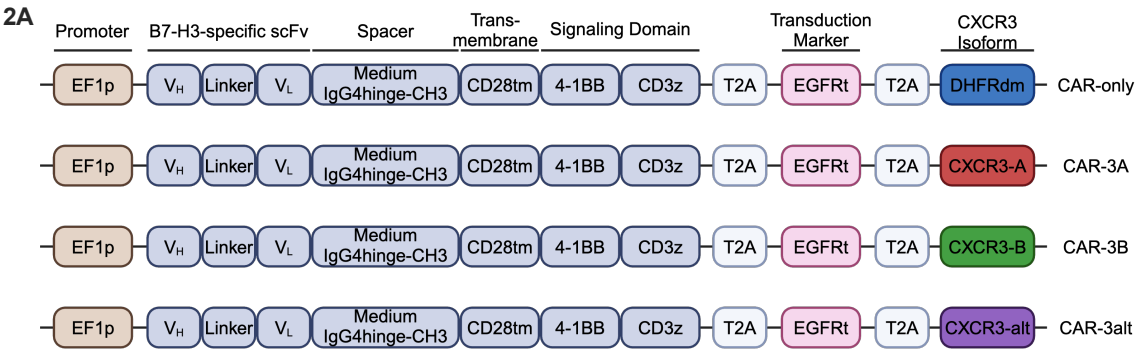
166
167

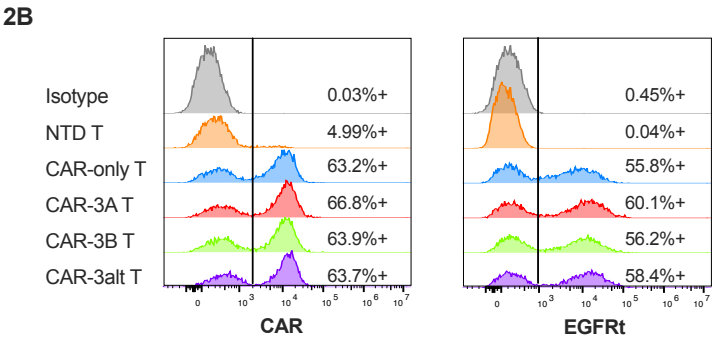
Figure 1. *B7-H3 CAR T cells are cytotoxic against patient-derived DIPG cells and able to produce CXCL10, which can induce chemotactic migration of CAR T cells that heterogeneously upregulate CXCR3.* (A) B7-H3 expression on primary DIPG cells (blue) by flow cytometry with isotype controls (red). (B) Relative cell viability of PBT-22FH or PBT-29FH cells after co-cultured with non-transduced (NTD) or CAR T cells at the indicated E:T ratios for 24 hours. (C) Concentrations of CXCL9, CXCL10, and CXCL11 by ELISA in co-cultures of NTD T or CAR T cells with PBT-22FH or PBT-29FH target cells at E:T of 1:1 for 24 hours. (D) CXCR3 expression on quiescent T cells, anti-CD3/CD28 beads-stimulated T cells, and generated CAR T cells by flow cytometry. (E) Percentage of CAR T cells that migrated from insert wells through 5-µm pores to bottom wells with CXCL10 at the indicated time points. (F) Relative cell viability of PBT-29FH cells after co-cultured with CXCL10-induced migrated CAR T cells for 24 hours. CAR T cells were seeded on insert wells to migrate through 5-µm pores to bottom wells with CXCL10 for 2 hours before removal of the insert wells. (G) Relative cell viability of PBT-29FH cells after cultured with CXCL10 for 24 hours. (H) Relative cell viability of PBT-29FH cells after directly co-cultured with CAR T cells at E:T of 1:1 in the presence of CXCL10 for 24 hours. Cell viability was normalized to the vehicle control without T cells in (B, F, G and H). p values were determined by two-way ANOVA with Sidak's multiple comparisons test (B) or one-way ANOVA with Dunnett's multiple comparisons test (C, E, F, G and H) using data from three or more independent experiments. Significance was compared with NTD T cells at each E:T ratio in (B). Results are presented as means ± SD in (B, C, E, F, G and H). ns, not significant; *$p < 0.05$; **$p < 0.01$; ***$p < 0.001$; ****$p < 0.0001$.

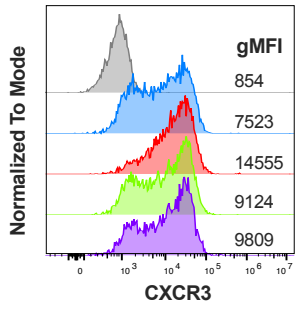
CXCR3-A-modified CAR T cells show enhanced migration toward CXCL10

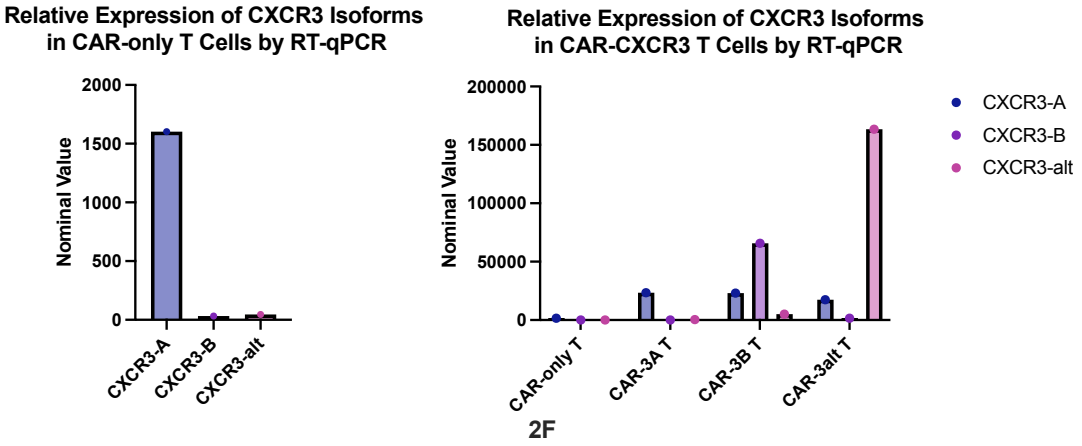
To test our hypothesis that engineering CAR T cells to overexpress CXCR3 can further sensitize CAR T cells to migrate toward CXCL10, we developed genetic constructs that allow co-expression of the B7-H3-specific CAR, a truncated epidermal growth factor receptor (EGFRt) transduction marker, and a CXCR3 isoform (Figure 2A). CXCR3 has three different isoforms in human due to alternative splicing[20], namely CXCR3-A, CXCR3-B, and CXCR3-alt, and we generated B7-H3 CAR T cells overexpressing each of these isoforms. While the CAR and EGFRt marker genes were consistently transduced and expressed on the surface across the CAR T cell groups (Figure 2B), the commercially available antibodies for CXCR3 could only detect elevated CXCR3 expression on the CXCR3-A-modified CAR T cells (CAR-3A) (Figure 2C), but not on the CAR T cells engineered to overexpress CXCR3-B (CAR-3B) or CXCR3-alt (CAR-3alt) in comparison to the unmodified CAR T cells (CAR-only). Therefore, we performed RT-qPCR to evaluate the relative RNA expression of each CXCR3 isoform. Our data suggest that CXCR3-A was the dominant isoform in the CAR-only T cells (Figure 2D, left panel), and CXCR3-A expression was exponentially increased in the CAR-3A T cells, while CXCR3-B and CXCR3-alt were specifically overexpressed in the CAR-3B and CAR-3alt T cells respectively (Figure 2D, right panel). Of note, the primer pairs to detect CXCR3-A had unavoidable overlaps with the CXCR3-B and CXCR3-alt sequences, which accounted for the artifacts of elevated CXCR3-A expression in the CAR-3B and CAR-3alt T cells.

To compare the migration efficiency of all the CXCR3-modified CAR T cells, we first performed the trans-well chemotaxis assay with CXCL10. Compared to the CAR-only T cells, the CAR-3A T cells showed significantly enhanced migration toward CXCL10; however, this was not observed with the CAR-3B or CAR-3alt T cells (Figure 2E). Based on the literature, it is controversial whether CXCR3-B promotes cell migration, and CXCR3-alt has been described to primarily interact with CXCL11 among the CXCR3 ligands[20,21]. To test the activity of the overexpressed CXCR3-alt in the CAR-3alt T cells, we then compared the CAR T cell migration toward CXCL11, and we demonstrated that both the CAR-3A and CAR-3alt T cell groups migrated more efficiently when induced by CXCL11 (Figure 2F). Although the CAR-3alt T cells may warrant further investigation, given the lack of production of CXCL11 by the CAR T cells (Figure 1C), we focused our study on the CAR-3A T cells for further development.


2A
Promoter
B7-H3-specific scFv
Spacer
Trans-membrane
Signaling Domain
Transduction Marker
CXCR3 Isoform
EF1p
VH
Linker
VL
Medium IgG4hinge-CH3
CD28tm
4-1BB
CD3z
T2A
EGFRt
T2A
DHFRdm
CAR-only
CXCR3-A
CAR-3A
CXCR3-B
CAR-3B
CXCR3-alt
CAR-3alt


2B
Isotype
NTD T
CAR-only T
CAR-3A T
CAR-3B T
CAR-3alt T
0.03%+
4.99%+
63.2%+
66.8%+
63.9%+
63.7%+
0.45%+
0.04%+
55.8%+
60.1%+
56.2%+
58.4%+
CAR
EGFRt


2C
Normalized To Mode
gMFI
854
7523
14555
9124
9809
CXCR3


2D
Relative Expression of CXCR3 Isoforms in CAR-only T Cells by RT-qPCR
Nominal Value
2000
1500
1000
500
0
CXCR3-A
CXCR3-B
CXCR3-alt
Relative Expression of CXCR3 Isoforms in CAR-CXCR3 T Cells by RT-qPCR
200000
150000
100000
50000
0
CAR-only T
CAR-3A T
CAR-3B T
CAR-3alt T
CXCR3-A
CXCR3-B
CXCR3-alt

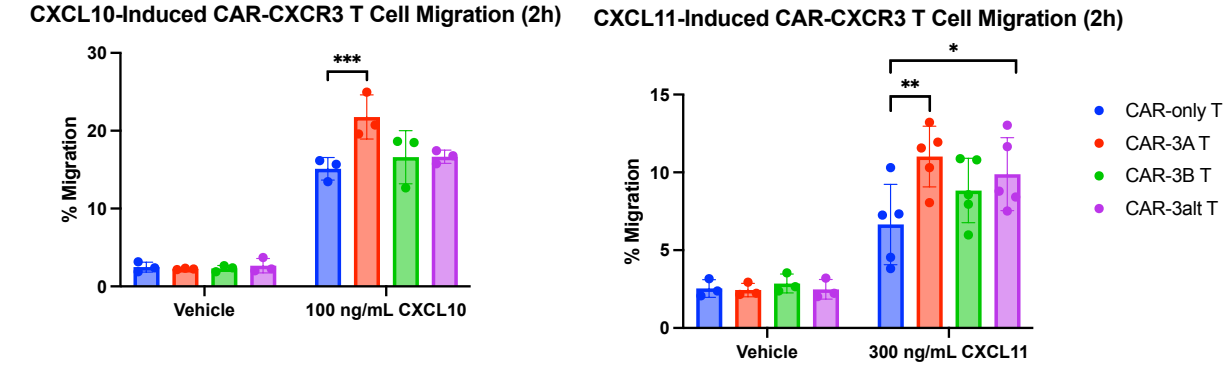

2E
CXCL10-Induced CAR-CXCR3 T Cell Migration (2h)
% Migration
30
20
10
0
***
Vehicle
100 ng/mL CXCL10
2F
CXCL11-Induced CAR-CXCR3 T Cell Migration (2h)
% Migration
15
10
5
0
**
*
Vehicle
300 ng/mL CXCL11
CAR-only T
CAR-3A T
CAR-3B T
CAR-3alt T

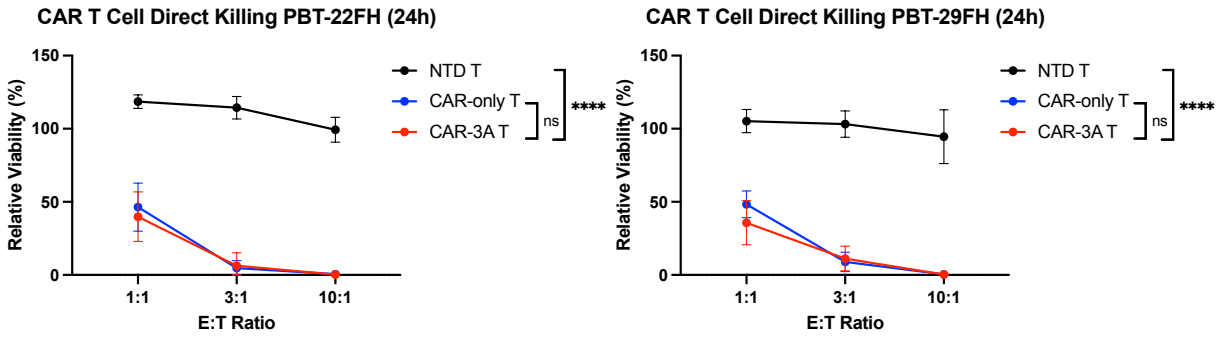
Figure 2. *CXCR3-A-modified CAR T cells show enhanced migration toward CXCL10.* (A) Illustration of constructs to generate B7-H3 CAR T cells that overexpress various isoforms of CXCR3. (B and C) CAR, EGFRt transduction marker, and CXCR3 expression on unmodified and CXCR3-modifed CAR T cells by flow cytometry. gMFI, geometric mean fluorescent intensity. (D) Relative expression of CXCR3 isoforms in unmodified or CXCR3-modifed CAR T cells by RT-qPCR. The data were normalized to β-actin control then nominally multiplied by 10^8 for data display. (E and F) Percentage of CAR T cells that migrated from insert wells to bottom wells with CXCL10 or CXCL11 after 2 hours. p values were determined by two-way ANOVA with Dunnett's multiple comparisons test (E and F) using data from three or more independent experiments. Results are presented as means ± SD in (E and F). ns, not significant; *$p < 0.05$; **$p < 0.01$; ***$p < 0.001$.

CXCR3-A-modified CAR T cells show enhanced migration and efficacy against DIPG across multiple T cell donors in response to CXCR3 ligands

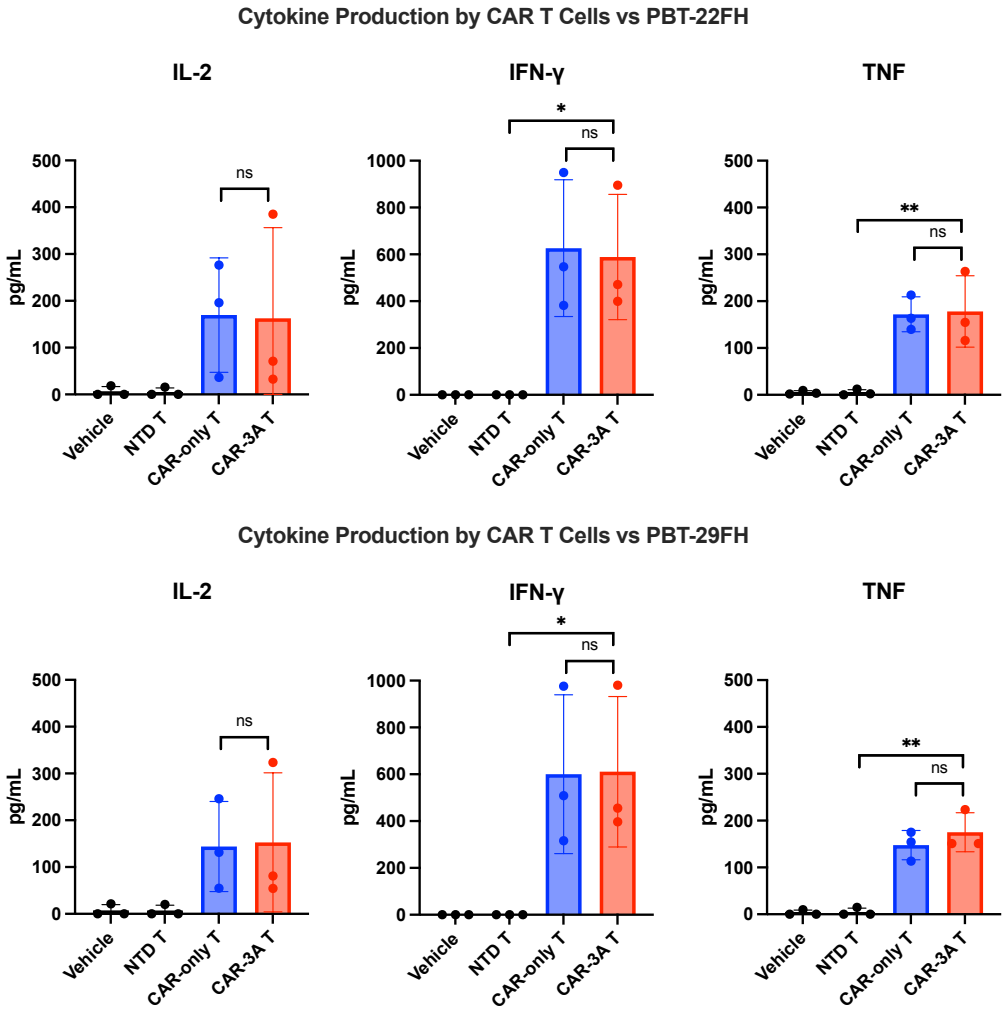
To validate our study results across multiple T cell donors, we generated the CXCR3-A-modified and unmodified B7-H3 CAR T cells with isolated T cells from three different PBMC donors. Despite donor variability, there was no significant difference between the CAR-3A and CAR-only T cells in terms of the fold expansion during production (Extended Data Fig. 1A), the CAR transduction rate (Extended Data Fig. 1B), the proportion of CD4 and CD8 T cells (Extended Data Fig. 1D), the distribution of T cell phenotypes (Extended Data Fig. 1E), as well as the expression of T cell exhaustion markers including PD1, TIM3, and LAG3 (Extended Data Fig. 1F), while the CXCR3 expression was elevated on the CAR-3A T cells (Extended Data Fig. 1C) across the three donors. Furthermore, we demonstrated that the CAR-3A and CAR-only T cells had similar cytotoxicity and cytokine production when they were directly co-cultured with the patient-derived DIPG cells in vitro (Figure 3A and 3B).

Next, we compared the migration efficiency of the CAR-3A and CAR-only T cells from the three T cell donors toward CXCR3 ligands including CXCL9, CXCL10, and CXCL11. In trans-well chemotaxis assays, the CAR-3A T cells showed enhanced migration toward all three ligands of CXCR3 (Figure 3C). We then performed the trans-well killing assay using DIPG cells cultured with CXCL9, CXCL10, or CXCL11. As shown in Figure 3D, despite some variations among the donors, when the migration was induced by CXCL9, CXCL10, or CXCL11, the CAR-3A T cells consistently resulted in more DIPG tumor death, when compared to the CAR-only T cells. This enhanced efficacy was corroborated by the increased cytokines produced by the migrated CAR-3A T cells (Figure 3E). As our data showed that the presence of CXCL9, CXCL10, or CXCL11 would not specifically enhance the cytotoxicity or cytokine production of the CAR-3A T cells when they were directly co-cultured with the DIPG cells in the control experiments (Figure 3F and 3G), we confirmed that the enhanced efficacy by the CAR-3A T cells in the trans-well killing assays (Figure 3D and 3E) should be attributed to their more efficient migration toward the CXCR3 ligands.

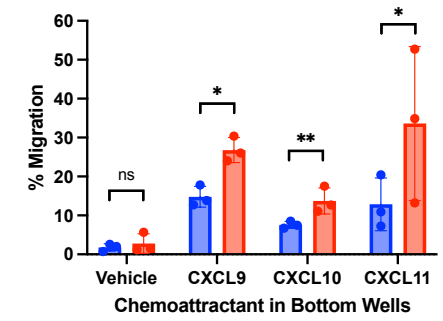
3A


CAR T Cell Direct Killing PBT-22FH (24h)
Relative Viability (%)
150
100
50
0
1:1
3:1
10:1
E:T Ratio
NTD T
CAR-only T
CAR-3A T
ns
****
CAR T Cell Direct Killing PBT-29FH (24h)
Relative Viability (%)
150
100
50
0
1:1
3:1
10:1
E:T Ratio
NTD T
CAR-only T
CAR-3A T
ns
****

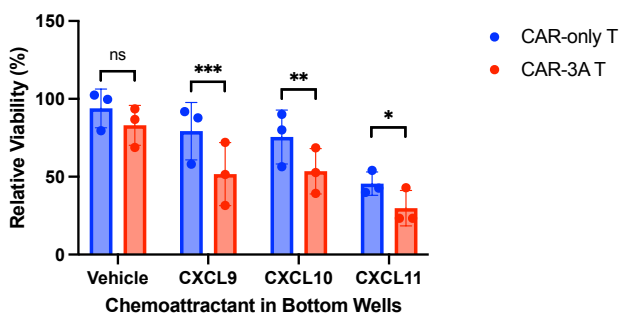
3B


Cytokine Production by CAR T Cells vs PBT-22FH
IL-2
pg/mL
500
400
300
200
100
0
ns
Vehicle
NTD T
CAR-only T
CAR-3A T
IFN-γ
pg/mL
1000
800
600
400
200
0
*
ns
Vehicle
NTD T
CAR-only T
CAR-3A T
TNF
pg/mL
500
400
300
200
100
0
**
ns
Vehicle
NTD T
CAR-only T
CAR-3A T
Cytokine Production by CAR T Cells vs PBT-29FH
IL-2
pg/mL
500
400
300
200
100
0
ns
Vehicle
NTD T
CAR-only T
CAR-3A T
IFN-γ
pg/mL
1000
800
600
400
200
0
*
ns
Vehicle
NTD T
CAR-only T
CAR-3A T
TNF
pg/mL
500
400
300
200
100
0
**
ns
Vehicle
NTD T
CAR-only T
CAR-3A T

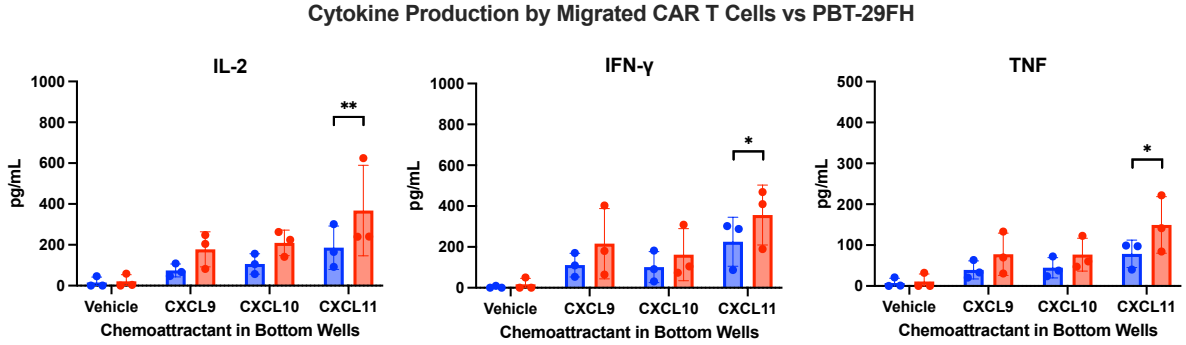
3C


CXCR3 Ligand-Induced CAR T Cell Migration (2h)
% Migration
60
50
40
30
20
10
0
ns
*
**
*
Vehicle
CXCL9
CXCL10
CXCL11
Chemoattractant in Bottom Wells

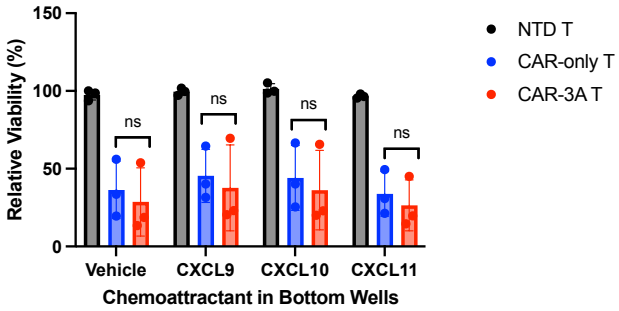
3D


PBT-29FH Viability (24h) with Migrated CAR T Cells
Relative Viability (%)
150
100
50
0
ns
***
**
*
Vehicle
CXCL9
CXCL10
CXCL11
Chemoattractant in Bottom Wells
CAR-only T
CAR-3A T

3E


Cytokine Production by Migrated CAR T Cells vs PBT-29FH
IL-2
pg/mL
1000
800
600
400
200
0
**
Vehicle
CXCL9
CXCL10
CXCL11
Chemoattractant in Bottom Wells
IFN-γ
pg/mL
1000
800
600
400
200
0
*
Vehicle
CXCL9
CXCL10
CXCL11
Chemoattractant in Bottom Wells
TNF
pg/mL
500
400
300
200
100
0
*
Vehicle
CXCL9
CXCL10
CXCL11
Chemoattractant in Bottom Wells

3F


PBT-29FH Viability (24h) with Chemoattractant
and Directly Added CAR T Cells
Relative Viability (%)
150
100
50
0
ns
ns
ns
ns
Vehicle
CXCL9
CXCL10
CXCL11
Chemoattractant in Bottom Wells
NTD T
CAR-only T
CAR-3A T

3G

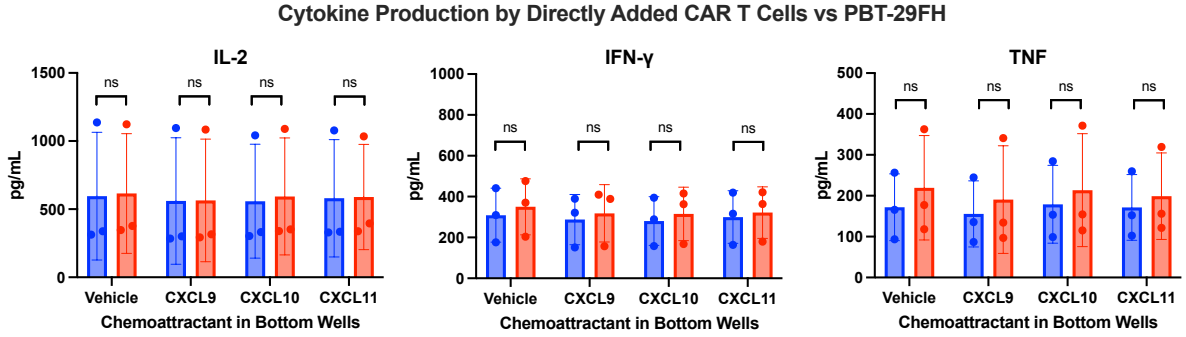

Cytokine Production by Directly Added CAR T Cells vs PBT-29FH
IL-2
pg/mL
1500
1000
500
0
ns
ns
ns
ns
Vehicle
CXCL9
CXCL10
CXCL11
Chemoattractant in Bottom Wells
IFN-γ
pg/mL
1000
800
600
400
200
0
ns
ns
ns
ns
Vehicle
CXCL9
CXCL10
CXCL11
Chemoattractant in Bottom Wells
TNF
pg/mL
500
400
300
200
100
0
ns
ns
ns
ns
Vehicle
CXCL9
CXCL10
CXCL11
Chemoattractant in Bottom Wells

Figure 3. *CXCR3-A-modified CAR T cells show enhanced migration and efficacy against DIPG across multiple T cell donors in response to CXCR3 ligands* (A) Relative cell viability of PBT-22FH or PBT-29FH cells after co-cultured with CAR T cells at the indicated E:T ratios for 24 hours. (B) Concentrations of IL-2, IFN-γ, and TNF by ELISA in co-cultures of CAR T cells with PBT-22FH or PBT-29FH target cells at E:T of 10:1 for 24 hours. (C) Percentage of CAR T cells that migrated from insert wells to bottom wells with vehicle, 300 ng/mL CXCL9, 100 ng/mL CXCL10, or 300 ng/mL CXCL11 after 2 hours (D) Relative cell viability of PBT-29FH cells after co-cultured with migrated CAR T cells for 24 hours. CAR T cells were seeded on insert wells to migrate to bottom wells with vehicle, 300 ng/mL CXCL9, 100 ng/mL CXCL10, or 300 ng/mL CXCL11 for 2 hours before removal of the insert wells. (E) Concentrations of IL-2, IFN-γ, and TNF by ELISA in cultures from (D) after 24 hours. (F) Relative cell viability of PBT-29FH cells after directly co-cultured with CAR T cells at E:T of 1:1 in the presence of vehicle, 300 ng/mL CXCL9, 100 ng/mL CXCL10, or 300 ng/mL CXCL11 for 24 hours. (G) Concentrations of IL-2, IFN-γ, and TNF by ELISA in cultures from (F) after 24 hours. Cell viability was normalized to the vehicle control without T cells in (A, D, and F). p values were determined by randomized block (matching the data for each donor) two-way ANOVA with Tukey's multiple comparisons test (A), randomized block one-way ANOVA with Dunnett's multiple comparisons test (B), or randomized block two-way ANOVA with Sidak's multiple comparisons test (C, D, E, F and G) using data from three different T cell donors. Results are presented as means ± SD. ns, not significant; *p < 0.05; **p < 0.01; ***p < 0.001; ****p < 0.0001.

Paracrine chemokines can lead to enhanced efficacy by CXCR3-A-modified CAR T cells against DIPG

As antigen-stimulated CAR T cells would produce CXCL9 and CXCL10 (Figure 1C), we investigated if the chemokines produced by CAR T cells from co-culturing with DIPG cells would be sufficient to induce CAR T cell migration in trans-well killing assays. We first prepared CAR T cell-conditioned medium by stimulating the B7-H3 CAR T cells with DIPG cells and harvesting the supernatant after 24 hours, then we applied the conditioned medium in a trans-well killing assay. As shown in Figure 4A, while the CAR T cell conditioned medium had some direct inhibitory effect on the DIPG cells, it induced the CAR-3A T cells to migrate and kill DIPG cells, as evidenced by the significantly more reduced tumor viability, which was also substantially lower (though not statistically significant) in comparison to the CAR-only T cell group.

Next, we tested whether the CAR-3A T cells would demonstrate enhanced efficacy in a long-term trans-well killing assay without exogenously added chemoattractant, in which seeded CAR T cells were given 24 hours to continuously migrate from the insert wells to the bottom wells with only DIPG cells (Figure 4B). Since some CAR T cells would pass through the insert pores in the absence of exogenous chemoattractant (Figure 1E), they would be stimulated by the DIPG cells and release chemokines including CXCL9 and CXCL10 in the bottom wells, which should attract more CAR T cells to actively migrate and in turn lead to more chemokine production as positive feedback in the following hours. Given that the CAR-3A T cells were more efficient migrating toward CXCL9 and CXCL10 than the CAR-only T cells, we hypothesized that more DIPG cells would be killed by the migrated CAR-3A T cells via the amplified positive feedback loop. Indeed, the CAR-3A T cells

consistently outperformed the CAR-only T cells in this assay, either in repeated experiments using CAR T cells of the same donor (Extended Data Fig. 2) or across all three T cell donors (Figure 4B), supporting our hypothesis.

Moreover, we investigated whether DIPG tumors would contribute to the paracrine CXCL10, as CXCL10 is inducible by IFN-γ[22], a major cytokine produced by stimulated CAR T cells (Figure 3B). As demonstrated in Figure 4C, while our primary DIPG cells would not make CXCL10 in the absence of IFN-γ, substantial amount of CXCL10 was produced by the DIPG cells when cultured with IFN-γ. Therefore, the production of CXCL10 can be reinforced by DIPG tumors in response to IFN-γ when treated by CAR T cells.

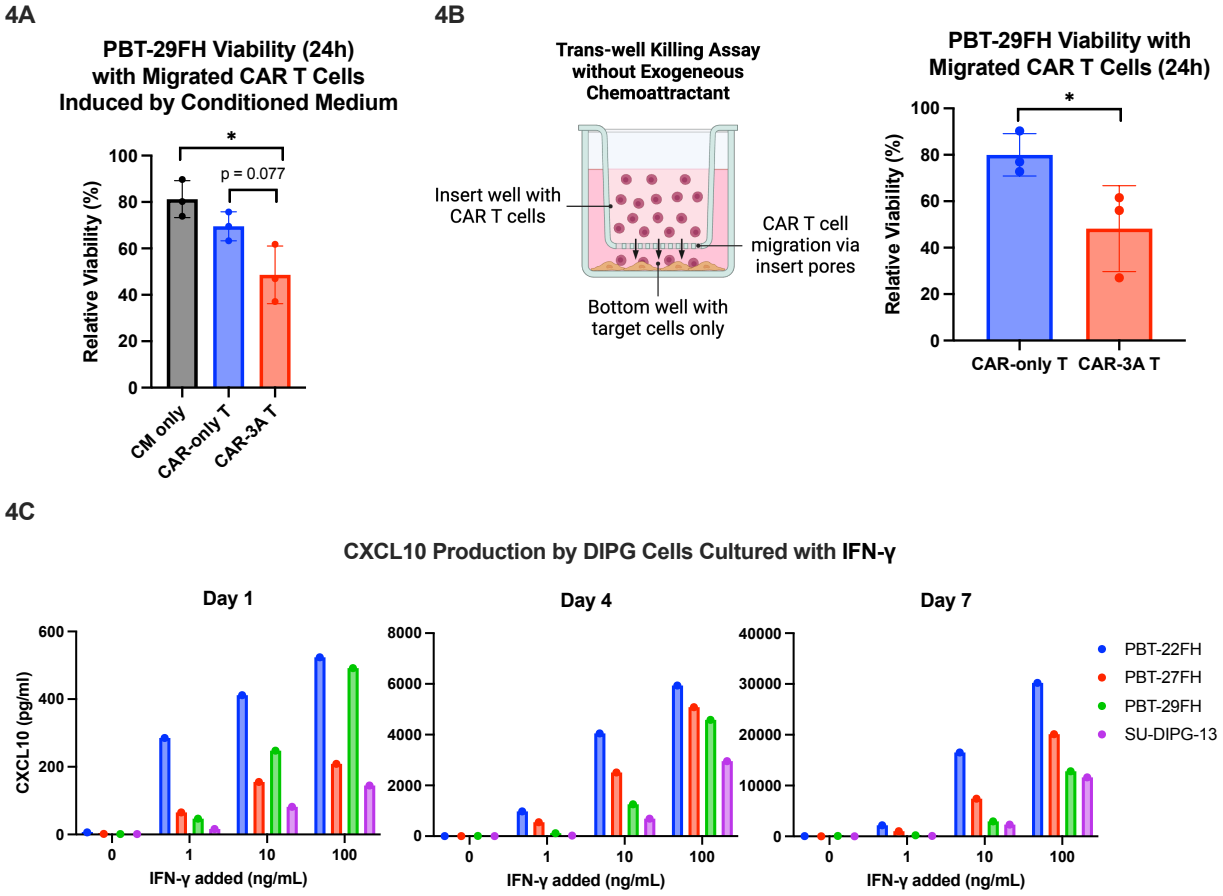


Figure 4. *Paracrine chemokines can lead to enhanced efficacy by CXCR3-A-modified CAR T cells against DIPG.* (A) Relative cell viability of PBT-29FH cells after co-cultured with migrated CAR T cells for 24 hours. CAR T cells were seeded on insert wells to migrate for 2 hours to bottom wells with conditioned medium (CM) from antigen-stimulated CAR T cell culture, before removal of the insert wells. (B) Relative cell viability of PBT-29FH cells after co-cultured with continuously migrating CAR T cells for 24 hours. CAR T cells were seeded on insert wells and allowed to migrate for 24 hours to bottom wells without chemoattractant. (C) Concentrations of CXCL10 by ELISA at the indicated time points in cultures of DIPG cells with added IFN-γ at the indicated doses. p

values were determined by randomized block (matching the data for each donor) one-way ANOVA with Dunnett's multiple comparisons test (A) or paired t test (B) using data from three different T cell donors. Results are presented as means ± SD in (A and B). *$p < 0.05$.

CXCR3-A-modified CAR T cells show enhanced trafficking and therapeutic efficacy when delivered intracerebroventricularly in orthotopic DIPG models

Based on our encouraging in vitro data, we investigated the effect of engineering CXCR3-A in CAR T cells against orthotopic DIPG mouse models. We first intracranially implanted luciferase-labeled SU-DIPG-13 cells into NSG mice, which is an aggressive and well-studied DIPG in vivo model[23]. As illustrated in Figure 5A, after 7 days, the mice were treated with the CAR-3A, CAR-only, or non-transduced (NTD) T cells of the same donor via either IV or ICV injection, as both routes have been used in clinical studies for pediatric CNS tumor patients. To compare CAR T cell trafficking from the periphery via IV or from the CSF via ICV to the tumor, we sacrificed mice from each treatment group at 24-hour and 48-hour time points to harvest the mouse brains. The IHC staining for human CD3, CD4, and CD8 indicated increased presence of the CAR-3A T cells around the tumor sites, compared with the CAR-only or NTD T cells, at both time points post-delivery to the mouse CSF through ICV injection (representative images shown in Figure 5B; additional images shown in Extended Data Fig. 3). In contrast, there was lack of T cell trafficking to the brain through IV administration during the first 48 hours (Extended Data Fig. 4). The tumor areas were defined based on H&E staining (Figure 5B and Extended Data Fig. 3 and 4) and confirmed by IHC staining for human Ki67 and B7-H3 (Extended Data Fig. 5).

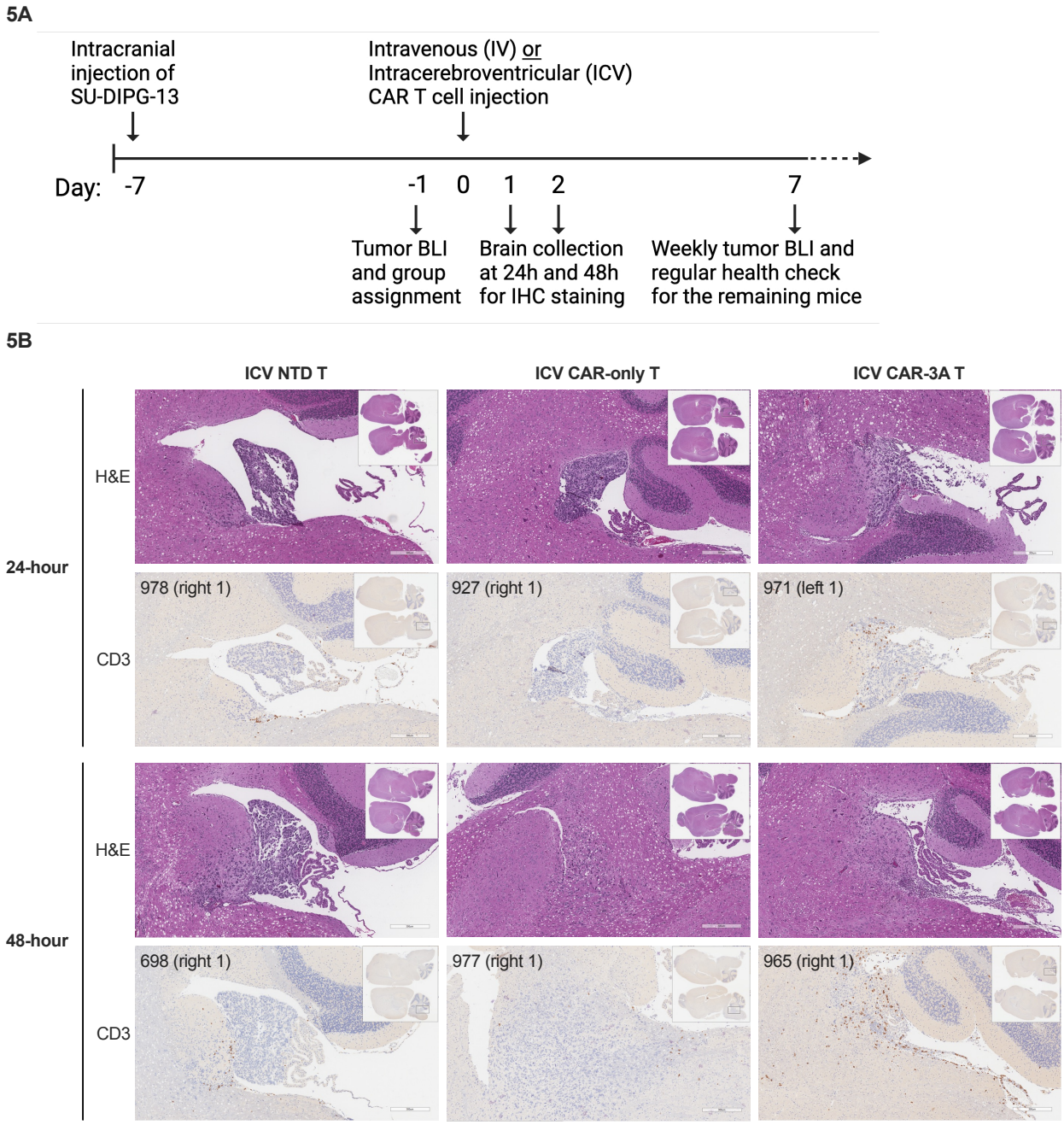


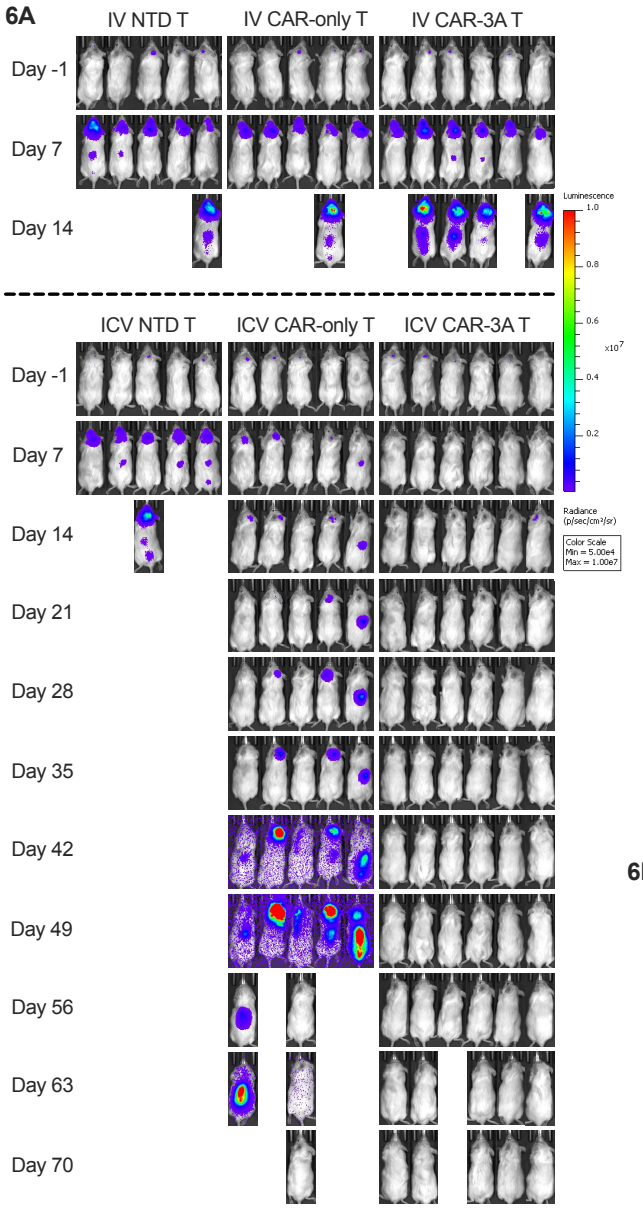
Figure 5. *CXCR3-A-modified CAR T cells show enhanced trafficking to the tumor site post ICV delivery in an orthotopic DIPG model.* (A) Illustration of the experimental plan (details described in the Methods section). (B) Representative images of H&E staining for the tumors and IHC staining for human CD3 around the corresponding tumor areas from the mouse brains collected on day 1 and day 2 (additional images shown in Extended Data Fig. 3).

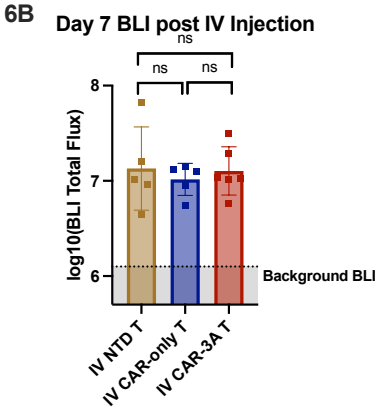
To compare the therapeutic efficacy of the CAR-3A and CAR-only T cells, bioluminescent imaging (BLI) was performed weekly for the remaining mice to measure the signals from the DIPG tumors. As SU-DIPG-13 cells could metastasize to the spinal cord (Figure 6A), we quantified the BLI signals from the whole body of the mice in this experiment. When the CAR T cells were locoregionally delivered via ICV injection, the CAR-3A T cells reduced the tumor signals to the background level within 7 days (Figure 6C) and maintained complete tumor regression in this study (Figure 6D). In contrast, although the ICV administered CAR-only T cells significantly inhibited the tumor growth compared to the NTD T cells (Figure 6C), rapid rebound of tumor signals from either the brain or the spinal cord was observed in 4 out of 5 mice from this group (Figure 6A and 6D), which led to their fatality based on protocol-defined euthanasia criteria (Figure 6E).

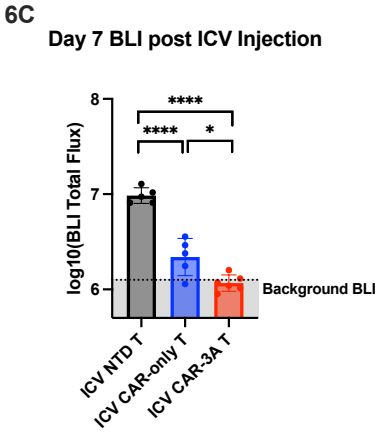
To be noted, prior to the end of this study, one mouse treated with ICV injected CAR-3A T cells met the euthanasia criteria without apparent tumor signal from previous BLI images (Figure 6A). H&E and IHC staining for the mouse brain showed presence of xenograft tumor (human Ki67+) yet with low expression of human B7-H3 (Extended Data Fig. 6), suggesting tumor antigen escape as a resistance mechanism under the selective pressure by the CAR-3A T cells. The fact that this coincided with loss of luciferase expression indicated that the tumor relapse was derived from a limited number of double-negative tumor cells, which could be addressed by CAR T cells with multiple specificities such as Seattle Children's ongoing trial (NCT05768880).

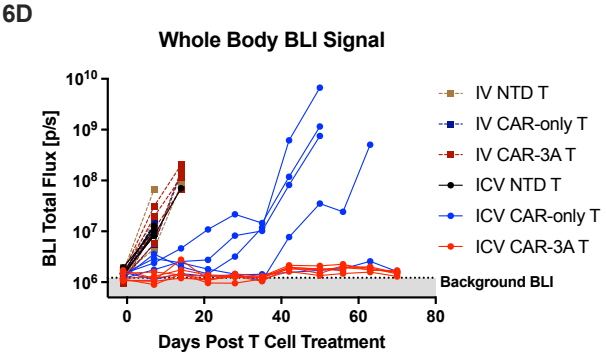
On the other hand, neither CAR T cell groups demonstrated efficacy when delivered systemically through IV injection (Figure 6A, 6B, 6D, and 6E), which was most likely due to the insufficient trafficking of CAR T cells from the periphery to the brain (Extended Data Fig. 4).

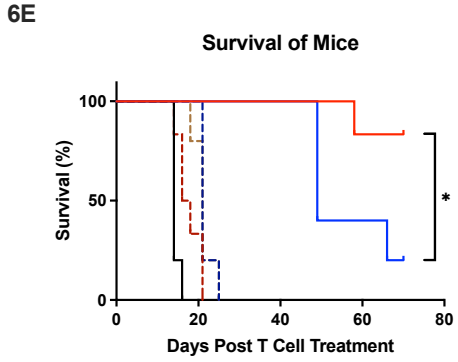
Mouse weight loss and neurologic symptoms were correlated with tumor progression (Figure 6F), and there was no evident toxicity by the CAR-3A T cells in comparison with the CAR-only T cells.

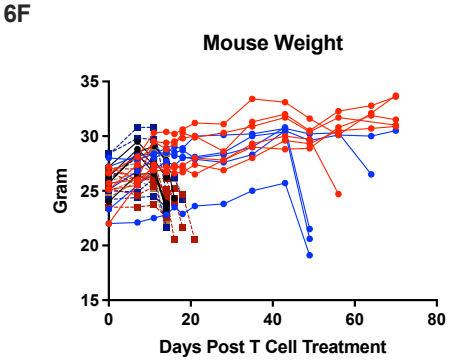

6A
IV NTD T
IV CAR-only T
IV CAR-3A T
Day -1
Day 7
Day 14
Luminescence
ICV NTD T
ICV CAR-only T
ICV CAR-3A T
Day -1
Day 7
Day 14
Day 21
Day 28
Day 35
Day 42
Day 49
Day 56
Day 63
Day 70
Radiance (p/sec/cm²/sr)
Color Scale
Min = 5.00e4
Max = 1.00e7


6B
Day 7 BLI post IV Injection
ns
ns
ns
log10(BLI Total Flux)
Background BLI
IV NTD T
IV CAR-only T
IV CAR-3A T


6C
Day 7 BLI post ICV Injection
****
****
*
log10(BLI Total Flux)
Background BLI
ICV NTD T
ICV CAR-only T
ICV CAR-3A T


6D
Whole Body BLI Signal
BLI Total Flux [p/s]
Background BLI
Days Post T Cell Treatment
IV NTD T
IV CAR-only T
IV CAR-3A T
ICV NTD T
ICV CAR-only T
ICV CAR-3A T


6E
Survival of Mice
Survival (%)
*
Days Post T Cell Treatment


6F
Mouse Weight
Gram
Days Post T Cell Treatment

399
400

Figure 6. *CXCR3-A-modified CAR T cells show enhanced therapeutic efficacy when ICV delivered in an orthotopic DIPG model.* (A) BLI images of mice at the indicated imaging time points. (B and C) Log_{10} of bioluminescent total flux from SU-DIPG-13 tumor cells in each mouse on day 7. (D) Bioluminescent total flux from SU-DIPG-13 tumor cells at the indicated time points. (E) Kaplan-Meier plot for mouse survival. (F) Mouse weight at the indicated time points. Results are presented as means ± SD in (B and C). p values were determined by one-way ANOVA with Tukey's multiple comparisons test (B and C) or log-rank (Mantel–Cox) test (E). ns, not significant; *p < 0.05; **p < 0.01; ***p < 0.001; ****p < 0.0001.

To validate these findings, we also evaluated the safety and efficacy of the CAR-3A T cells in a second DIPG in vivo model and used T cells from another donor. In brief, luciferase-labeled PBT-27FH cells were intracranially engrafted in NSG mice for 35 days before T cell administration through ICV injection (Extended Data Fig. 7A). The BLI signals from the mouse brain suggested substantial decrease in tumor burden by the CAR-3A T cells within 7 days of treatment (Extended Data Fig. 7B), indicating efficient tumor engagement by the CAR-3A T cells. while the tumor signals remained above baseline in most mice treated with the CAR-only T cells. Despite the extended time for the tumor to progress in this model (Extended Data Fig. 7C and 8), the mice treated with the CAR-3A T cells had survival advantage compared to the mice in the NTD or CAR-only T cell groups (Extended Data Fig. 7D), though the comparison to the latter did not reach statistical significance. To be noted, the statistical power of this study was unexpectedly reduced, because two mice in the CAR-3A T cell group without tumor BLI signal (Extended Data Fig. 8) were euthanized per requests by the veterinary staff due to non-tumor related causes (vaginal prolapse, day 182; bacterial infection, day 193). IHC staining for human Ki67 and B7-H3 confirmed absence of tumor in these brains (Extended Data Fig. 9). There was no weight loss (Extended Data Fig. 7E) or sign of illness such as lethargy, hunching posture at rest, or hair loss exhibited by the mice in relation to the treatment of the CAR-3A T cells, supporting the safety of this CAR T cell engineering approach.

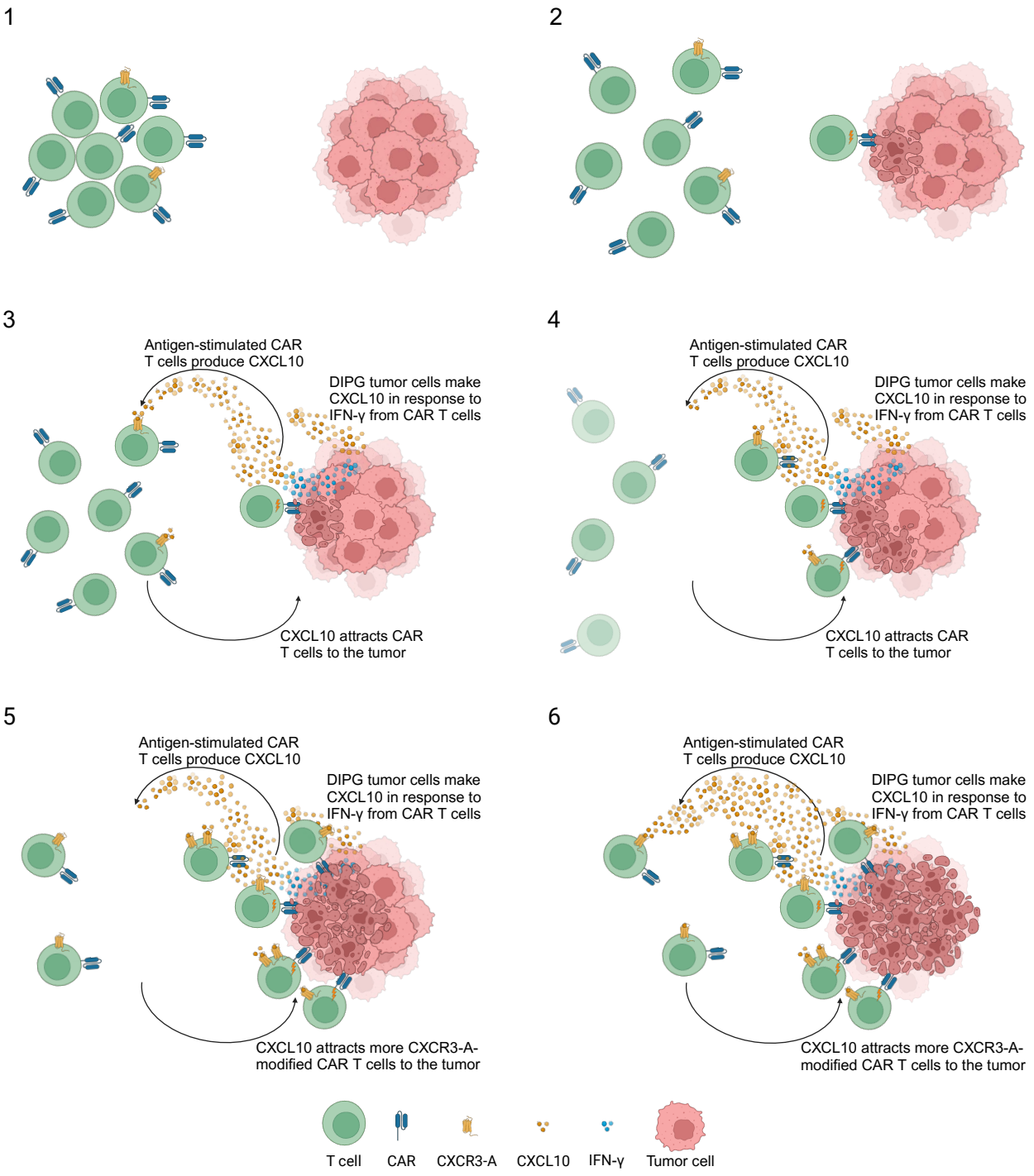


Figure 7. *Schematic of the proposed working model.* (1 and 2) Some of the ICV delivered CAR T cells encounter tumor and get stimulated by the tumor antigen, leading to some tumor cell death. (3 and 4) The stimulated CAR T cells produce chemokines such as CXCL10, which can recruit additional CAR T cells that endogenously express CXCR3. DIPG tumor cells also express CXCL10 in response to IFN-γ released by stimulated CAR T cells. (5) By engineering the CAR T cells to overexpress CXCR3-A, more CAR T cells respond and migrate to the tumor site. (6) This effect in

turn results in more CXCL10 production, followed by more CAR T cell recruitment through positive feedback, which lead to more tumor cell death, thus improving the trafficking and efficacy of CAR T cell therapies for DIPG.

Discussion:

As DIPG is universally fatal and responsible for nearly 25,000 years of lost potential life each year in the US alone[2,3], more effective treatments are desperately needed. Here, we developed a new iteration of CAR T cell therapy by engineering B7-H3 CAR T cells to overexpress CXCR3-A, in order to improve CAR T cell trafficking to the tumor. We demonstrate that, compared to the standard B7-H3 CAR T cell therapy, our CXCR3-A-modified CAR T cells migrate more efficiently toward the CXCR3 ligands (e.g. CXCL10) in vitro and show enhanced trafficking and therapeutic efficacy when delivered intracerebroventricularly in our orthotopic DIPG mouse models. Because CXCL10 is produced by activated CAR T cells as well as by DIPG cells in response to IFN-γ from activated CAR T cells, this CXCL10 could attract more CXCR3-A-modified CAR T cells to migrate to the tumor, which would result in a positive feedback loop by amplifying the CXCL10 production and further recruitment of CAR T cells, thus leading to improved therapeutic efficacy against DIPG (Figure 7).

It is worth noting that while the tumor microenvironment (TME) of DIPG has been described as immunologically inert[24,25], other immune cells in the CNS such as microglia could be attracted and in turn contribute to the chemokine and cytokine production in the TME following CAR T cell administration, which may reinforce a pro-inflammatory environment and further recruit other anti-tumor immune cells. However, the interactions between CAR T cells and other immune cell types need to be studied in immuno-competent syngeneic DIPG mouse models with murine CAR T cells, which has its own limitations and is out of the scope of this manuscript.

Our clinical data with the standard B7-H3 CAR T cells indicated some CAR T cell activity and elevated CXCL10 in the CSF of patients with DIPG[7,8], which may be sufficient to initiate the positive feedback loop for recruiting the CXCR3-A-modified CAR T cells. Nevertheless, our approach could further synergize with strategies that promote the production of CXCR3 ligands from the tumor cells prior to CAR T cell administration, to increase the initial tumor engagement by the CXCR3-A-modified CAR T cells. For example, oncolytic virus encoding a CXCL11 gene has been preclinically developed[26], which could target tumor cells to express CXCL11 and attract more CXCR3-A-modified CAR T cells immediately after the injection. In addition, since DIPG cells would make CXCL10 in response to IFN-γ, oncolytic virus encoding an IFN-γ gene may provide a similar effect for enhancing the trafficking of the CXCR3-A-modified CAR T cells as a combination therapy for DIPG.

Preclinical evidence, including results in this study, has suggested the superiority of locoregional CAR T cell delivery to the CNS over systemic dosing in treating CNS tumor models[27-29], and CAR T cell clinical trials for CNS tumors have demonstrated feasibility and tolerability of injecting CAR T cells to the CNS of patients[4,15]. As such, it is important to study CAR T cell trafficking by administering CAR T cells to the CNS space in preclinical in vivo models. To our knowledge, we are the first to demonstrate that CAR T cell trafficking to the CNS tumor can be enhanced by engineering chemokine receptor expression in the CAR T cells when they are ICV delivered.

While our study focused on enhancing the B7-H3 CAR T cell therapy for DIPG, this concept of CXCR3-A-modified CAR T cells is readily applicable to CAR T cell therapies targeting other types of

solid tumor, provided with modifications of the CAR specificities for suitable tumor antigens. In addition, we focused on the CXCR3 isoform CXCR3-A for CAR T cell engineering based on our preliminary data and due to the lack of clinical data regarding the CXCL11 levels in the CAR T cell-treated DIPG patients. Nonetheless, the CXCR3-alt-modified CAR T cells could be beneficial in tumor context where CXCL11 production is relevant.

Of note, the role of CXCR3-B in cell migration has been conflicting based on the current literature[20,21]. As CXCR3 only has one isoform in mouse, which is the counterpart for CXCR3-A in human, CXCR3-B as well as CXCR3-alt have not been well studied. Here, our data suggested that CXCR3-B overexpression did not significantly increase T cell migration toward CXCL10 or CXCL11 (Figure 2E and 2F). However, the overexpression of CXCR3-B was only confirmed by RT-qPCR (Figure 2D), and we were not able to validate the surface expression of the transduced CXCR3-B due to the absence of commercially available antibody.

We showed enhanced trafficking and efficacy by the CXCR3-A-modified CAR T cells despite the fact that the unmodified CAR T cells upregulate CXCR3 expression due to the activation step in the commonly adopted production process (Figure 1D). However, as new CAR T cell production protocols are developed, some of which either omit the activation step to preserve the stemness of the CAR T cells[30] or generate CAR T cells through inducible pluripotent stem cells (iPSCs) for potential off-the-shelf applications[31], in these cases, engineering the CAR T cells to overexpress CXCR3 may be even more essential to promote CAR T cell trafficking and efficacy, as CAR T cells generated by these methods would have less endogenous CXCR3 expression.

Although the ability to assess the toxicity of a new CAR T cell therapy is limited in xenograft mouse models, we did not observe any safety concern derived from the engineering of CXCR3-A in the B7-H3 CAR T cells. Given the significantly enhanced therapeutic efficacy demonstrated in our study, CXCR3-A-modified CAR T cells deserve further preclinical and clinical investigations against DIPG and other solid tumors.

Materials and Methods:

Primary human DIPG cell culture

Human cell cultures were generated with informed consent in compliance with institutional review board approval at Seattle Children's Hospital (#14449). PBT-22FH, PBT-27FH, and PBT-29FH were biopsy-derived at diagnosis. For PBT-22FH, PBT-27FH, and PBT-29FH, tumor tissue was obtained at Seattle Children's Hospital, and cell cultures were created at Fred Hutchinson Cancer Center as previously described[19]. SU-DIPG-13 was autopsy-derived and generously donated by Dr. Michael Monje (Stanford University). Cells were modified by lentiviral transduction followed by blasticidin selection (Fisher Scientific, #A1113903) to steadily express firefly luciferase. Cells were maintained in NeuroCult NS-A Basal Medium with NS-A Proliferation Supplement (Stemcell Technologies, #5751), 1x Antibiotic/Antimycotic (ThermoFisher Scientific, #15-240-062), 40 ng/mL epidermal growth factor (PeproTech, #AF-100-15), and 40 ng/mL fibroblast growth factor (PeproTech, #AF-100-18B). All cell culture models were validated by DNA fingerprinting and routinely tested to be mycoplasma negative.

CAR constructs

The medium-spacer human B7-H3-specific CAR construct has previously been described[7]. In brief, the CAR is comprised of a scFv derived from the MGA 271 monoclonal antibody, a medium-length spacer of IgG4-hinge-CH3, a CD28 transmembrane domain, a 4-1BB co-stimulatory domain, and a CD3ζ signaling domain, and the CAR sequence was appended to a T2A ribosomal skip sequence followed by a truncated EGFR (EGFRt) marker gene, which was appended to a second T2A sequence followed by the methotrexate-resistant human DHFR mutein gene, the last of which was not utilized in this paper. For the CAR constructs co-expressing a CXCR3 isoform, the human DHFR mutein gene was replaced with the open reading frame sequence of CXCR3-A, CXCR3-B, or CXCR3-alt (synthesized by Genewiz).

Lentiviral vector preparation

Lentiviral vectors were produced by transfecting Lenti-X 293-T cells (Takara, #632180), kindly provided by Dr. Bernasconi (University of Bern). In brief, 293-T cells were seeded in T150 flasks that were pre-coated with collagen (Millipore Sigma, #C3867-1VL) and cultured in DMEM medium (Gibco, #11960044) supplemented 10% fetal bovine serum (Gibco, #A5256701), 10 mM HEPES (Gibco, #15630080), 100 U/mL penicillin/streptomycin (Gibco, #15140122), and 1x GlutaMax (Gibco, #35050061) to grow to 80% confluence, after which the cells were incubated briefly with a cocktail of 3 mL of Opti-MEM (Gibco, #31985070) with 90 µL Lipofectamine 3000 transfection reagent (Invitrogen, # L3000015) that was gently mixed with 15 µg of the vector plasmid of interest and the packaging plasmids of 18 µg of psPAX2 (Addgene, #12260) and 7 µg of pCMV-VSV-G (Addgene, #8454). Additional culture medium was added thereafter. After culturing the transfected 293-T cells for 24 h and 48 h, supernatants that contained lentiviral vectors were collected and filtered through 0.45-mm syringe filters (Millipore Sigma, #SLHP033RS), then centrifuged at 18,000 x g for 20 h at 4 °C. The pellets of lentiviral vectors were resuspended in 2 mL of culture medium, aliquoted, and stored at -80 °C.

Generation of human CAR T cells

Bulk human T cells were isolated from peripheral blood mononuclear cells of healthy donors (Bloodworks Northwest) by negative selection using EasySep Human T Cell Isolation Kit (StemCell, #17951) and maintained in RPMI 1640 medium (Gibco, #21870076) supplemented 10% fetal bovine serum (Gibco, #A5256701), 10 mM HEPES (Gibco, #15630080), 100 U/mL penicillin/streptomycin (Gibco, #15140122), GlutaMax (Gibco, #35050061), 5 ng/mL recombinant human IL-7 (Biolegend, # 581904), and 0.5 ng/mL recombinant human IL15 (Biolegend, # 570304). Following isolation, T cells were stimulated with anti-CD3/CD28 Dynabeads (Gibco, #40203D) in the medium at 1 x 106 cells/mL for 24 h and transduced at a multiplicity of infection of 3, after which the transduced T cells were enumerated by a Vi-CELL BLU counter (Beckman Coulter) every other day and fed with the medium to 0.8 x 10^6 cells/mL density. After the expansion, the cells were cryopreserved in CryoStor CS10 (StemCell, #07930) until further use. To resuscitate cryopreserved cells, the cells were quickly thawed with pre-warmed medium and pelleted by centrifugation, then cultured in the medium overnight to recover, and the viable cell number was decided by a Vi-CELL BLU counter (Beckman Coulter) before being used for functional assays.

RT-qPCR

The RNA was extracted from cells using RNeasy Plus Mini Kit (QIAGEN, #74134) and converted to cDNA with High-Capacity RNA-to-cDNA kit (AppliedBiosystems, #4387406). The cDNA was then set up with TB Green (Takara, #RR42LR) and a primer pair (Integrated DNA Technologies) in four replicate wells for qPCR with Light Cycler 480 II (Roche). The expression of the gene of interest was normalized to the expression of actin, then multiplied by a nominal factor for data display.

Flow cytometry

For flow cytometry, the antibodies used included mouse-anti-human B7-H3-PE (BioLegend, clone MIH42, #351004), mouse-anti-human CXCR3-FITC (BioLegend, clone G025H7, #353704), mouse-anti-human EGFR-PE (BioLegend, clone AY13, #352904), mouse-anti-human CD4-PE (BioLegend, clone OKT4, #317410), mouse-anti-human CD8-APC (BioLegend, clone RPA-T8, #301049), mouse-anti-human CD45RA-PE (BioLegend, clone HI100, #304108), mouse-anti-human CD62L-BV421 (BioLegend, clone DREG-56, #304828), mouse-anti-human PD1-APC (BioLegend, clone A17188B, #621610), mouse-anti-human TIM3-APC (BioLegend, clone A18087E, #364804), mouse-anti-human LAG3-APC (BioLegend, clone 7H2C65, #369212), and biotinylated Protein L (GenScript, #M00097) followed by streptavidin-PE (BioLegend, #405204) secondary staining to detect the B7-H3-specific CAR expression. For flow cytometry analysis, cells were sampled and washed with PBS (Gibco, #10010023), incubated with antibodies in PBS on ice in darkness for 30 min, washed again with PBS twice, followed by secondary staining with additional wash steps when necessary, then evaluated on a LSR Fortessa (BD Biosciences) or Novocyte 3000 (Agilent) flow cytometer. The cell-surface expression of the proteins of interest was analyzed by FlowJo (Tree Star).

Luciferase assay

The primary DIPG cell lines used for luciferase assays were modified to express firefly luciferase. D-Luciferin (Revvity, #122799-5) substrate solution was added to the cell culture at the indicated time points for each assay and incubated at room temperature for 15 min before quantifying the bioluminescent signal from each well with a SpectraMax iD5 (Molecular Devices). All the in vitro

viability assays were performed three times or with T cells from three different donors, and the bioluminescent signals were normalized to the vehicle-treated control wells as 100% viability.

ELISA

ELISA assays were performed with DuoSet ELISA kits (R&D Systems) to detect CXCL9 (#DY392), CXCL10 (#DY266), CXCL11 (#DY672), IL-2 (#DY202), TNF (#DY210), and IFN-γ (#DY285B) concentrations in the collected supernatants per the manufacturer's instructions.

Trans-well chemotaxis assay

Trans-well chemotaxis assays were performed with Transwell 24-well Plate with 5.0 μm Pore Polycarbonate Membrane Insert (Corning, #3421) to assess the migration efficiency of CAR T cells toward chemoattractant. In brief, blank medium (vehicle) or medium with chemoattractant was added to the bottom wells, then the same number of CAR T cells was seeded on the insert wells, which allow active T cell migration through the pores to the bottom wells. After the indicated length of incubation, the number of migrated CAR T cells in each bottom well was counted in duplicates with Vi-CELL BLU counter (Beckman Coulter). All the trans-well chemotaxis assays were performed at least three times or with T cells from three different donors, and percent migration was calculated as the migrated cell number over the seeded cell number.

Trans-well killing assay

Trans-well killing assays were performed with Transwell 24-well Plate with 5.0 μm Pore Polycarbonate Membrane Insert (Corning, #3421). In brief, luciferase-labeled DIPG tumor cells were seeded in the bottom wells, then blank medium (vehicle) or medium with chemoattractant was added to the bottom wells. The same number of CAR T cells was seeded on the insert wells, which allow active T cell migration through the pores to the bottom wells. After 2-hour incubation, the insert wells were removed, and the plate was further incubated overnight to allow the migrated CAR T cells to kill the seeded DIPG tumor cells. At 24-hour time point, luciferase assay was performed as described above to quantify the viability of the seeded DIPG tumor cells. All the trans-well killings assays were performed three times or with T cells from three donors, and the bioluminescent signals were normalized to the vehicle-treated control wells as 100% viability. The chemoattractants used in this study include recombinant human CXCL9 (#ab283902), CXCL10 (#ab280332), and CXCL11 (#ab283901) from Abcam, as well as conditioned media harvested from co-cultures of CAR T cells and DIPG tumor cells.

Mouse experiments

All mouse experiments were conducted in accordance with the IACUC-approved protocol ACUC00669 at Seattle Children's Research Institute. For the orthotopic xenograft model with SU-DIPG-13, eight-week-old male NSG mice (Jackson Laboratories) were intracranially injected with 50,000 SU-DIPG-13 cells in 2 μL PBS (Cytiva, #SH30256.LS) using a stereotactic surgical setup with the coordinates of 0.8 mm lateral and 1.5 mm posterior from lambda, and 2.5 mm deep. Seven days after tumor implantation, 2 x 10^6 CAR T cells in 5 μL PBS were injected into the lateral ventricle of brain with the coordinates of 1.2 mm lateral and 0.6 mm posterior from bregma, and 2.0mm deep, or intravenously in 200 μL PBS. Mice were anesthetized by intraperitoneal injected cocktail of Ketamine (Patterson Veterinary Supply, #07-894-8462; 100 mg/kg animal) and Xylazine

(Patterson Veterinary Supply, #07-808-1947; 8 mg/kg animal) for the surgeries and given the painkiller of buprenorphine (Wedgewood Connect, #BUPREN-INJ010VC; 1 mg/kg animal, extended release) by the veterinary staff before the surgeries. Mice from each treatment group were euthanized at 24-hour and 48-hour post-treatment time points to collect their brains, which were used for immunohistochemistry (IHC) analysis to evaluate the migration of T cells toward the tumor site as describe below. For the rest of the mice in each treatment group, bioluminescent imaging (BLI) was performed weekly to measure the tumor signals, for which mice were anesthetized with isoflurane (Patterson Veterinary Supply, #07-890-8115), subcutaneously injected with D-luciferin (Revvity, #122799-5) substrate solution and imaged with IVIS Spectrum Imaging System (Perkin Elmer) after 15 min. Mouse weight was recorded on a weekly basis with routine health checks to monitor any sign of illness such as weight loss, hair loss, cranial distension, lethargy, and hunching posture at rest. Mice with severe symptoms were euthanized based on protocol-defined criteria, followed by collection of brains, livers, and spleens for IHC analysis.

For the experiment with PBT-27FH, gender-balanced NSG mice were intracranially injected with 350,000 PBT-27FH cells in 2 µL PBS using a stereotactic surgical setup with the same coordinates as described above. 35 days after tumor implantation, 1 x 10^5 CAR T cells in 3 µL PBS were injected into the lateral ventricle of the brain with the coordinates as described above. BLI was performed to measure the tumor signals. Mouse weight was recorded with routine health checks to monitor any sign of illness, and mice with severe symptoms were euthanized based on protocol-defined criteria, followed by collection of brains, livers, and spleens for IHC analysis if needed.

Tissue processing, IHC, and histopathologic analysis

Mouse brains were fixed in 10% neutral buffered formalin (Fisher Scientific, #57-35) for 24-72 hours, then transferred into 70% ethanol for long-term storage. Wet tissues were submitted to the Microscopy and Histopathology CoLab at Seattle Children's Research Institute for paraffin embedding. Formalin-fixed paraffin-embedded blocks were then submitted to the Experimental Histopathology lab at Fred Hutchinson Cancer Research Center for further processing. Tissue sections were cut 4-5 µm thick for Hematoxylin-Eosin (H&E) stains and IHC. IHC stains included human CD3 (Fisher Scientific, #RM9107S, 1:300), human CD4 (Millipore Sigma, #104R-26, 1:100), human CD8 (Agilent, #M7103, 1:200), human B7H3 (Abcam, #ab219648, 1:5000), human Ki67 (Cell Signaling, #12202, 1:1000), and Albumin (Genetex; #GTX102419, 1:2000) with a hematoxylin counterstain. H&E and IHC images were produced with an Aperio AT slide scanner.

Statistical analysis

The statistical analyses were performed as noted in the figure legends using Prism 10 (GraphPad) to determine the p values. Significance is reported if $p < 0.05$ (marked by an asterisk).

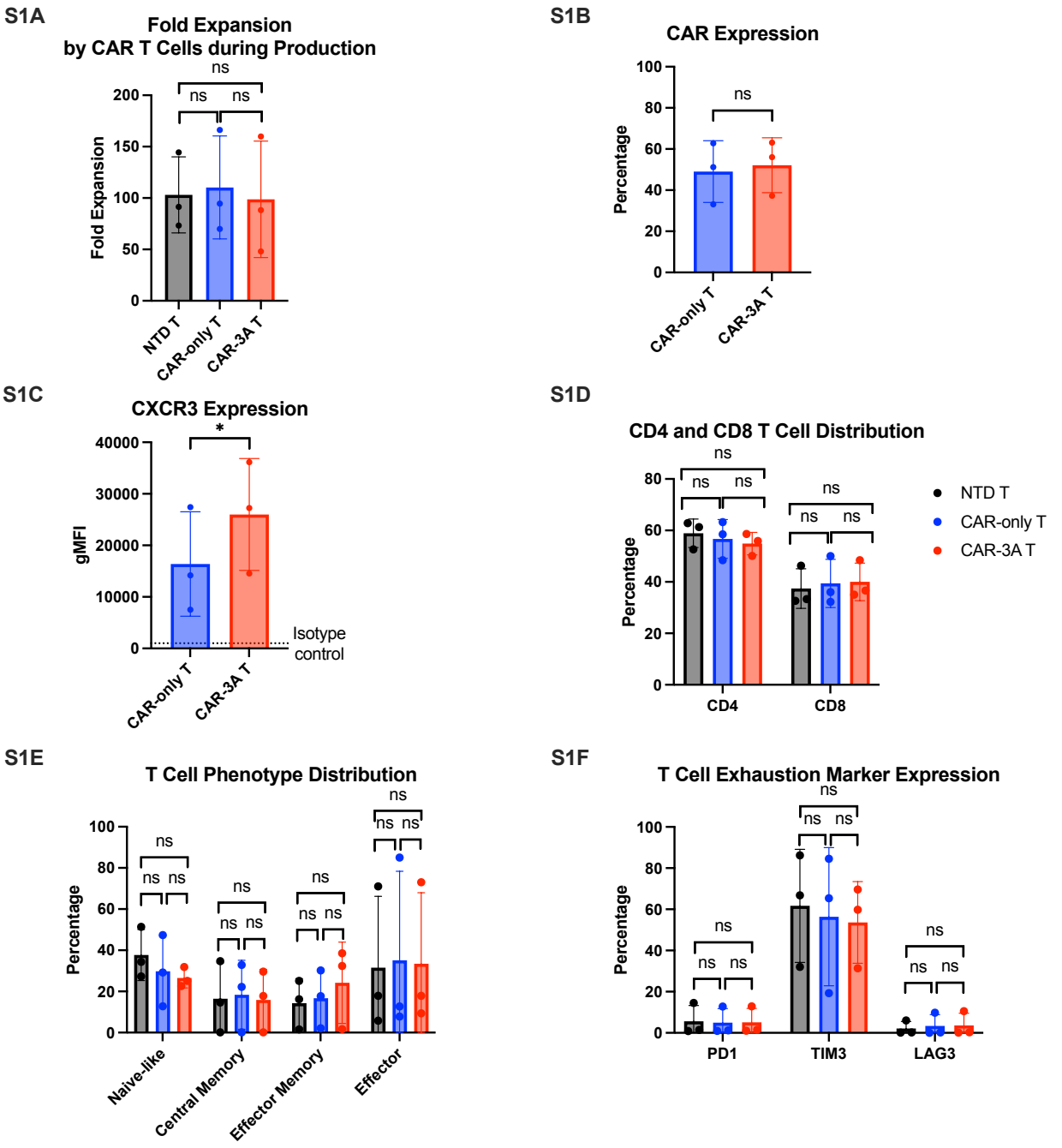
Illustrations

The illustrations and schematics in this manuscript were created in https://BioRender.com

Data availability

The data generated in this study are available upon request from the corresponding author.

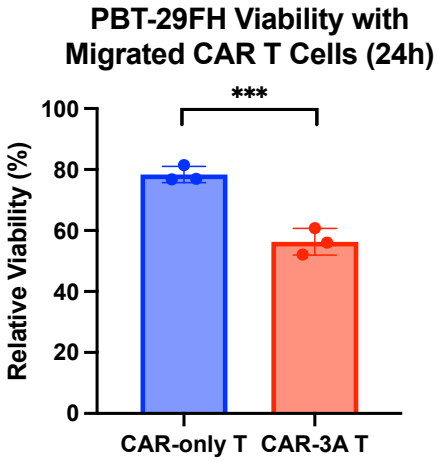
Extended Data:



Extended Data Figure 1. *CXCR3-A-modified CAR T cells show similar phenotypes as unmodified CAR T cells across three T cell donors.* (A) Fold expansion by CAR T cells during production. (B) Percentage of CAR expression on unmodified and CXCR3-A-modifed CAR T cells by flow cytometry. (C) Geometric mean fluorescent intensity of (gMFI) of CXCR3 on unmodified and CXCR3-A-modifed CAR T cells by flow cytometry. (D) Percentage of CD4 and CD8 T cell subset of generated CAR T cells. (E) Percentage of naïve-like (CD62L+/CD45RA+), central memory (CD62L+/CD45RA-),

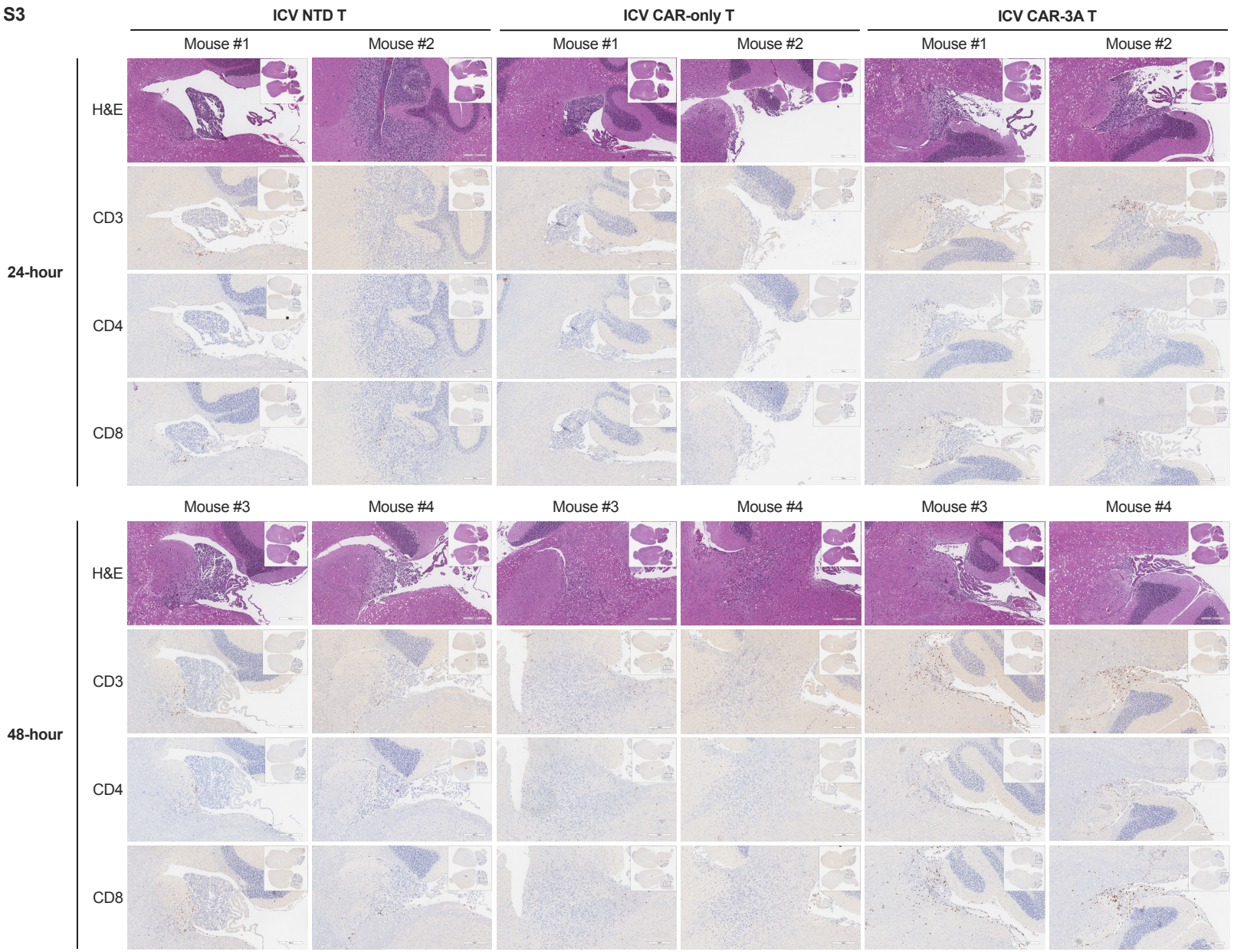
effector memory (CD62L-/CD45RA-), and effector (CD62L-/CD45RA+) subset of generated CAR T cells. (F) Percentage of the exhaustion markers PD1, TIM3, and LAG3 expression on generated CAR T cells. p values were determined by randomized block (matching the data for each donor) one-way ANOVA with Tukey's multiple comparisons test (A, D, E, and F) or paired t test (B and C) using data from three different T cell donors. Results are presented as means ± SD. ns, not significant, *p < 0.05.

S2



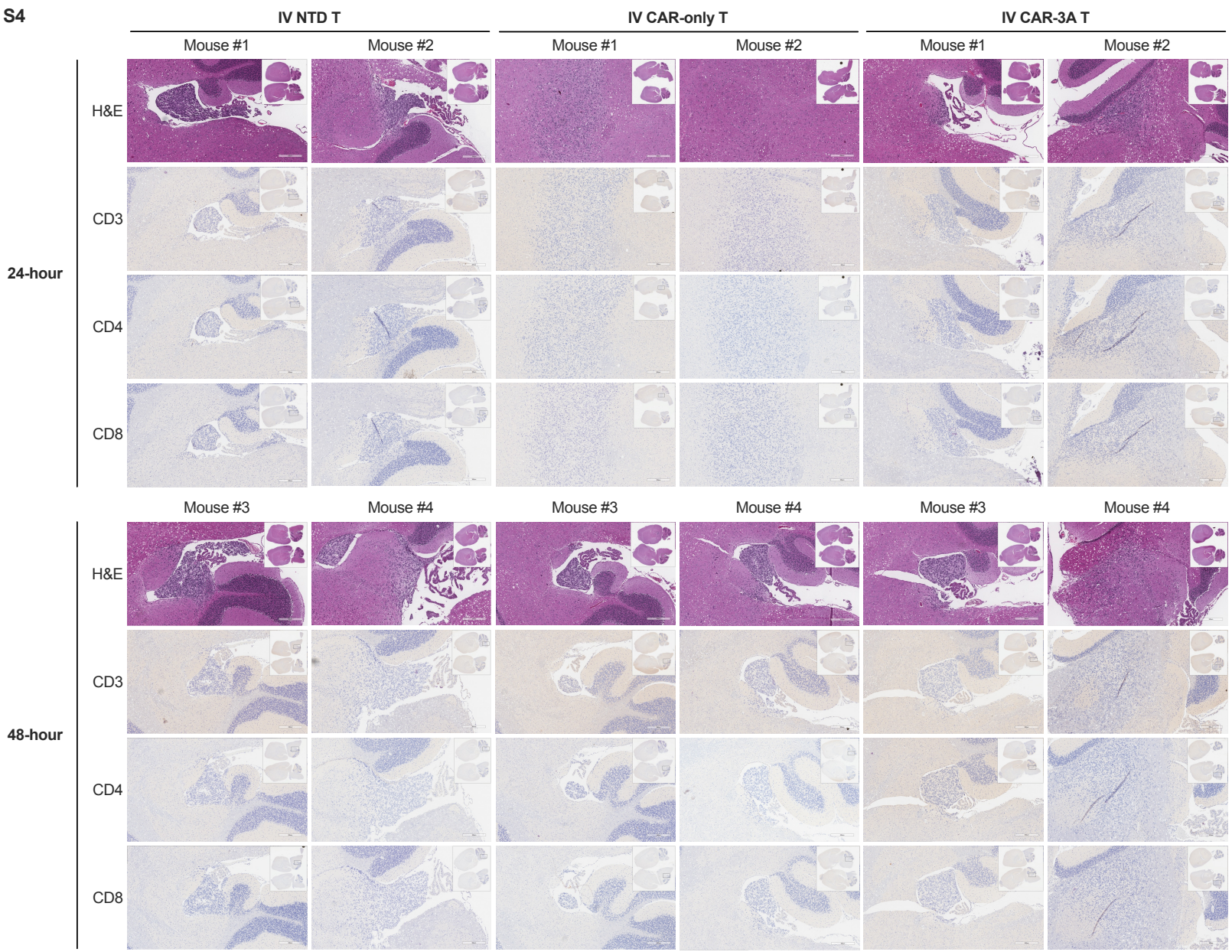
Extended Data Figure 2. *Paracrine chemokines can lead to enhanced efficacy by CXCR3-A-modified CAR T cells against DIPG.* Relative cell viability of PBT-29FH cells after co-cultured with continuously migrating CAR T cells for 24 hours. CAR T cells were seeded on insert wells to migrate for 24 hours to bottom wells without chemoattractant. p values were determined by unpaired t test using data from three independent experiments. Results are presented as means ± SD. ***p < 0.001.

S3

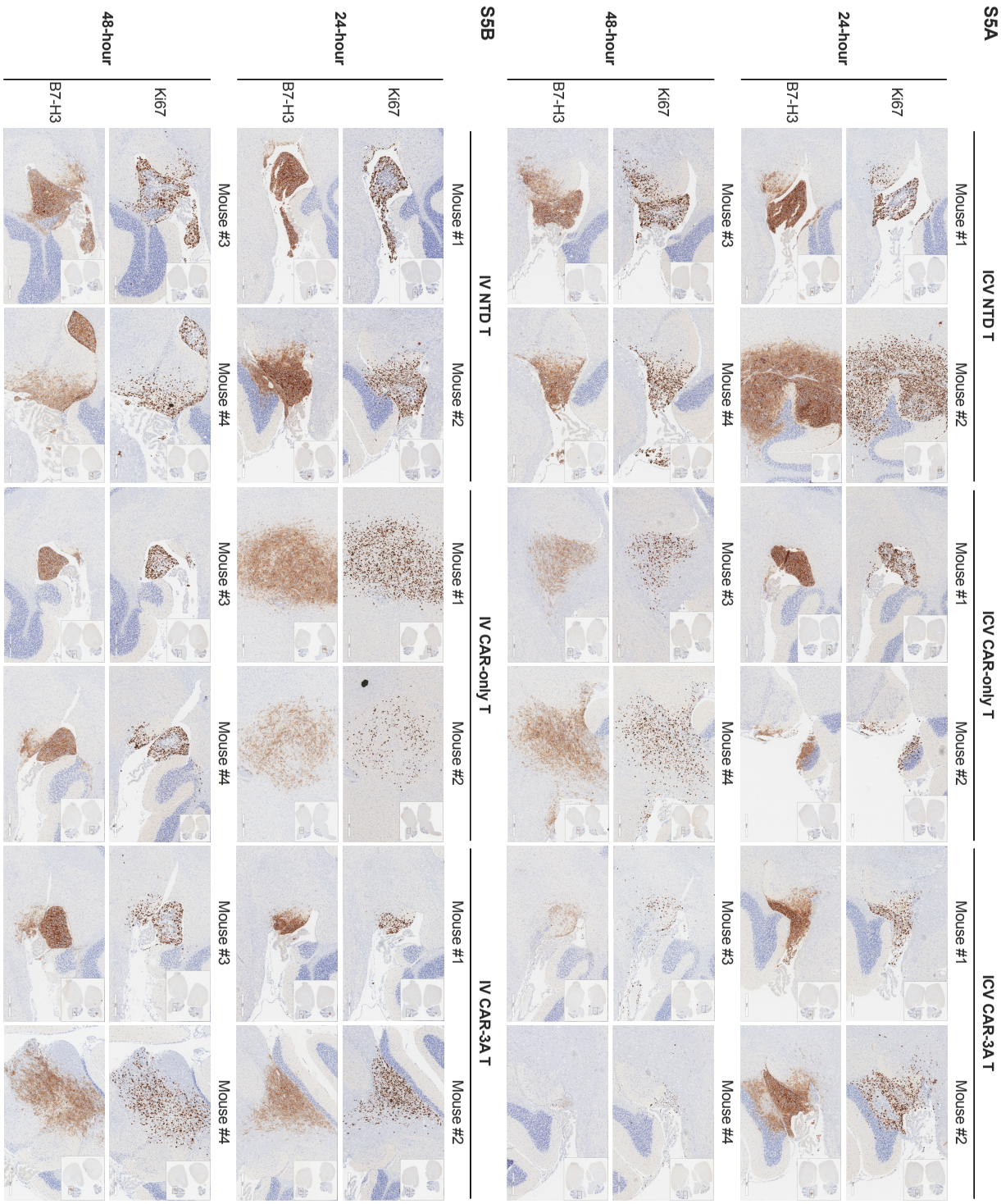

ICV NTD T
ICV CAR-only T
ICV CAR-3A T
Mouse #1
Mouse #2
Mouse #1
Mouse #2
Mouse #1
Mouse #2
24-hour
H&E
CD3
CD4
CD8
Mouse #3
Mouse #4
Mouse #3
Mouse #4
Mouse #3
Mouse #4
48-hour
H&E
CD3
CD4
CD8

Extended Data Figure 3. *CXCR3-A-modified CAR T cells show enhanced trafficking to the tumor site post ICV delivery in an orthotopic DIPG (SU-DIPG-13) model.* Representative images of H&E staining for the tumors and IHC staining for human CD3, CD4, and CD8 around the corresponding tumor areas from the mouse brains collected on day 1 and day 2, as illustrated in Figure 5A.

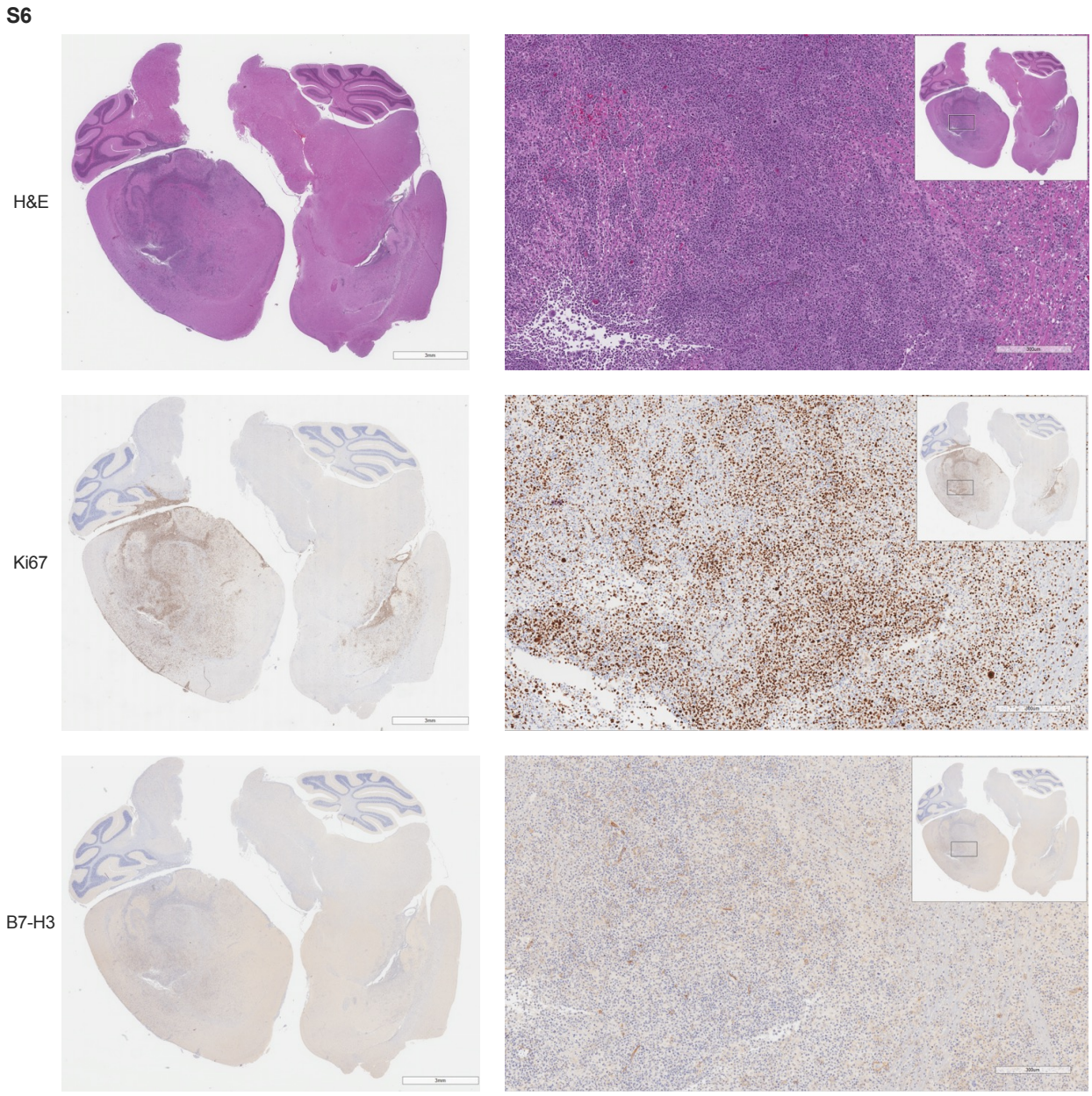
S4


IV NTD T
IV CAR-only T
IV CAR-3A T
Mouse #1
Mouse #2
Mouse #1
Mouse #2
Mouse #1
Mouse #2
24-hour
H&E
CD3
CD4
CD8
Mouse #3
Mouse #4
Mouse #3
Mouse #4
Mouse #3
Mouse #4
48-hour
H&E
CD3
CD4
CD8

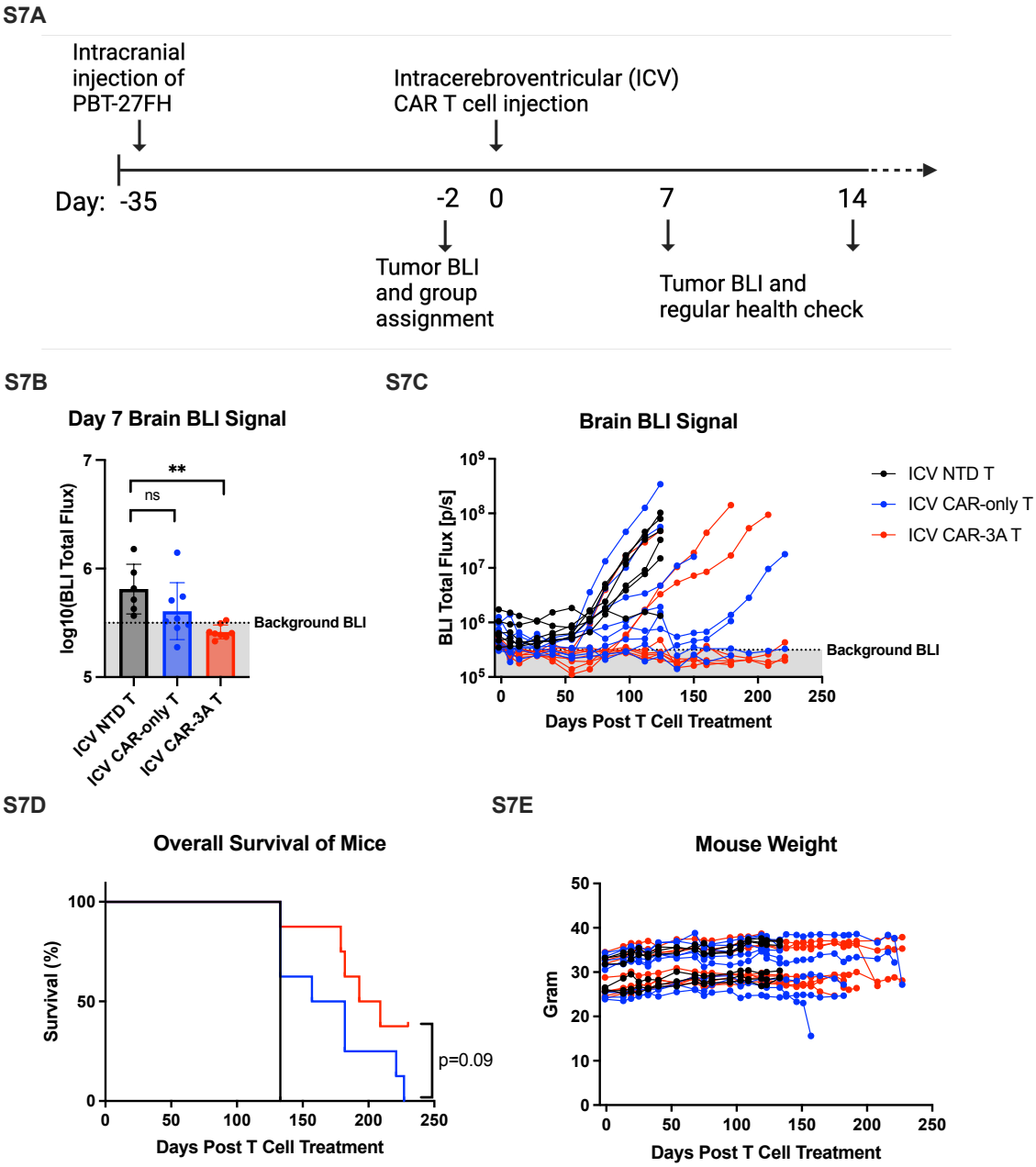
Extended Data Figure 4. *CAR T cells show lack of trafficking to the mouse brain post intravenous delivery in an orthotopic DIPG (SU-DIPG-13) model.* Representative images of H&E staining for the tumors and IHC staining for human CD3, CD4, and CD8 around the corresponding tumor areas from the mouse brains collected on day 1 and day 2, as illustrated in Figure 5A.



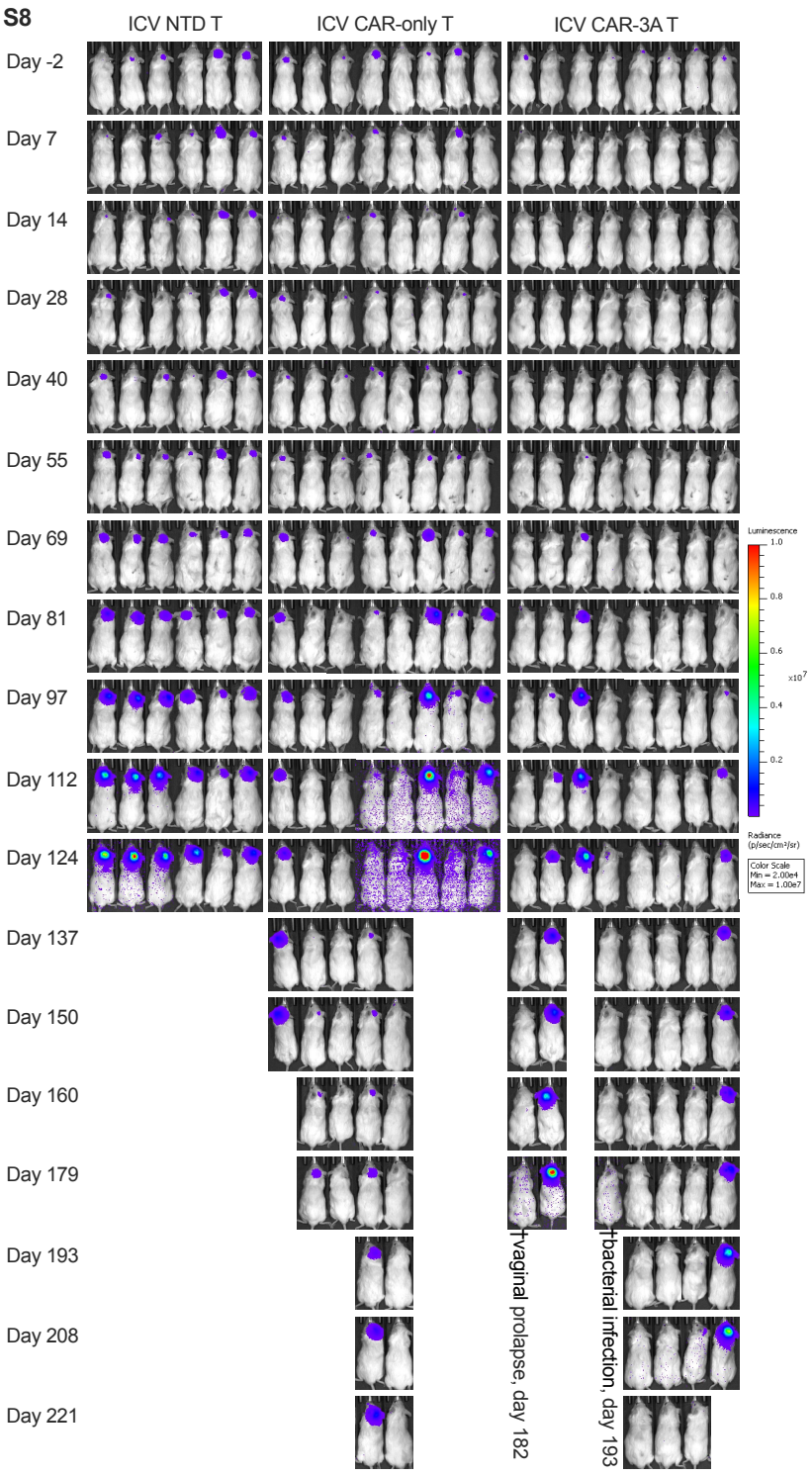
744
745
746 **Extended Data Figure 5.** *IHC staining for human Ki67 and B7-H3 confirms the tumor areas.*
747 Representative images of IHC staining for human Ki67 and B7-H3 around the focused areas (A)
748 for ICV groups in Extended Data Figure 3 and (B) for IV groups in Extended Data Figure 4.
749
750



Extended Data Figure 6. *H&E and IHC staining for human Ki67 and B7-H3 suggests tumor antigen escape.* Representative images of H&E and IHC staining for human Ki67 and B7-H3 from the mouse brain after relapse post ICV CAR-3A T cell treatment in Figure 6.

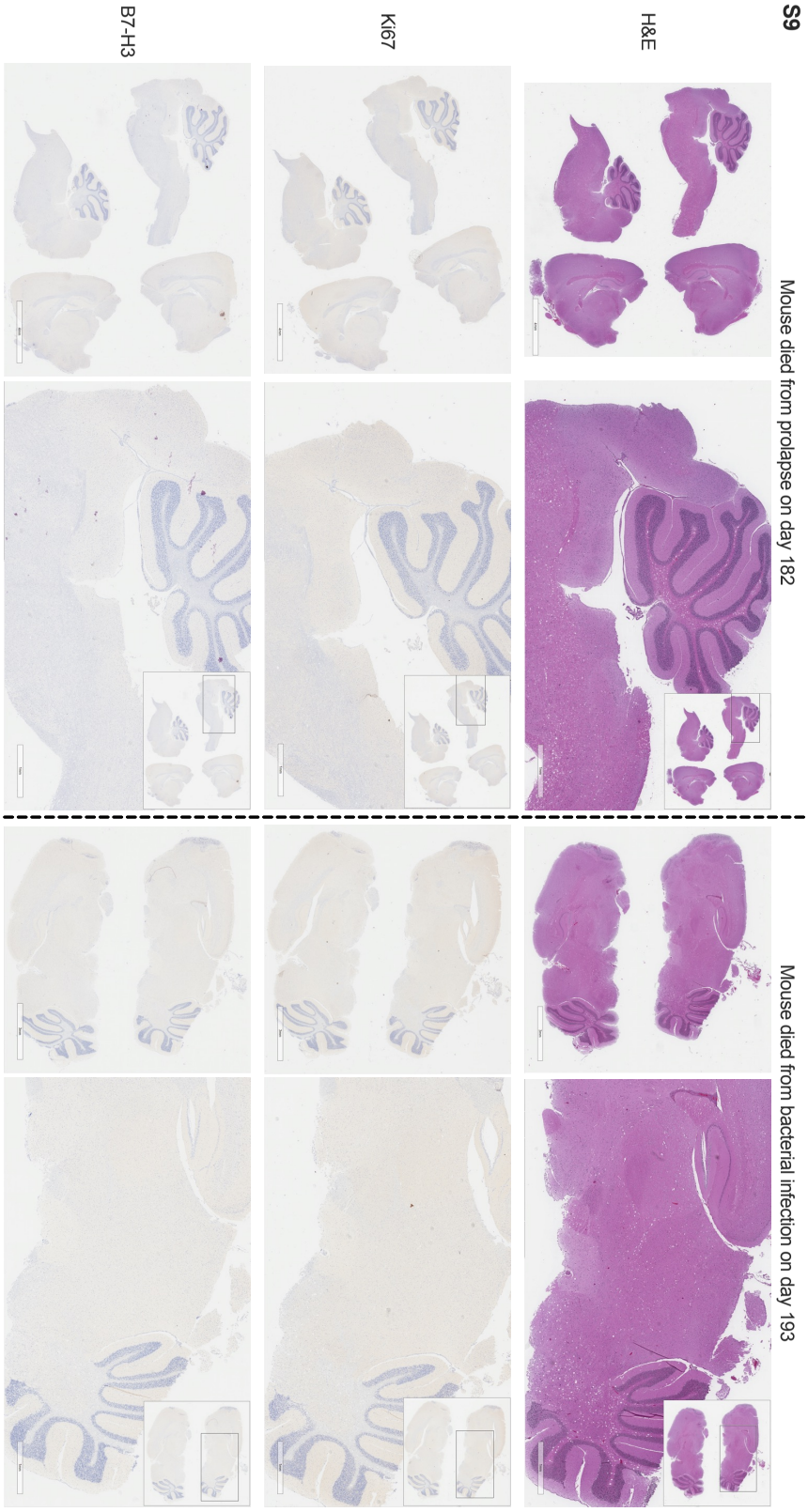


Extended Data Figure 7. *CXCR3-A-modified CAR T cells of another T cell donor show enhanced therapeutic efficacy when ICV delivered in a second orthotopic DIPG model.* (A) Illustration of the experimental plan (details described in the Methods section). (B) Log_{10} of bioluminescent total flux from PBT-27FH tumor cells in each mouse on day 7. (C) Bioluminescent total flux from PBT-27FH tumor cells at the indicated time points. (D) Kaplan-Meier plot for mouse overall survival that includes non-tumor related causes of death. (E) Mouse weight at the indicated time points. Results are presented as means ± SD in (B). p values were determined by one-way ANOVA with Tukey's multiple comparisons test (B) or log-rank (Mantel–Cox) test (D). ns, not significant; **p < 0.01.



Extended Data Figure 8. *CXCR3-A-modified CAR T cells of another T cell donor show enhanced therapeutic efficacy when ICV delivered in the second orthotopic DIPG (PBT-27FH) model.* BLI images of mice at the indicated imaging time points from the study shown in Extended Data Figure 7. †Non-tumor related causes of death and dates as noted in the results section.

777


S9
H&E
Ki67
B7-H3
Mouse died from prolapse on day 182
Mouse died from bacterial infection on day 193

778
779

Extended Data Figure 9. *H&E and IHC staining for human Ki67 and B7-H3 confirms absence of tumor.* Representative images of H&E and IHC staining for human Ki67 and B7-H3 from the brains of the two mice in the CAR-3A T cell group of Extended Data Figure 7, who were euthanized due to non-tumor related causes in the absence of tumor BLI signal.

References:

1 Siegel, R. L., Miller, K. D., Wagle, N. S. & Jemal, A. Cancer statistics, 2023. *CA Cancer J Clin* **73**, 17-48 (2023). https://doi.org:10.3322/caac.21763

2 Cooney, T. *et al.* Contemporary survival endpoints: an International Diffuse Intrinsic Pontine Glioma Registry study. *Neuro Oncol* **19**, 1279-1280 (2017). https://doi.org:10.1093/neuonc/nox107

3 Vitanza, N. A. & Monje, M. Diffuse Intrinsic Pontine Glioma: From Diagnosis to Next-Generation Clinical Trials. *Curr Treat Options Neurol* **21**, 37 (2019). https://doi.org:10.1007/s11940-019-0577-y

4 Ronsley, R. *et al.* CAR T cell therapy for pediatric central nervous system tumors: a review of the literature and current North American trials. *Cancer Metastasis Rev* (2024). https://doi.org:10.1007/s10555-024-10208-4

5 Uslu, U. & June, C. H. Beyond the blood: expanding CAR T cell therapy to solid tumors. *Nat Biotechnol* (2024). https://doi.org:10.1038/s41587-024-02446-2

6 Ferreras, C. *et al.* Facing CAR T Cell Challenges on the Deadliest Paediatric Brain Tumours. *Cells* **10** (2021). https://doi.org:10.3390/cells10112940

7 Vitanza, N. A. *et al.* Intraventricular B7-H3 CAR T Cells for Diffuse Intrinsic Pontine Glioma: Preliminary First-in-Human Bioactivity and Safety. *Cancer Discov* **13**, 114-131 (2023). https://doi.org:10.1158/2159-8290.CD-22-0750

8 Vitanza, N. A. *et al.* Intracerebroventricular B7-H3-targeting CAR T cells for diffuse intrinsic pontine glioma: a phase 1 trial. *Nat Med* (2025). https://doi.org:10.1038/s41591-024-03451-3

9 Karin, N. CXCR3 Ligands in Cancer and Autoimmunity, Chemoattraction of Effector T Cells, and Beyond. *Front Immunol* **11**, 976 (2020). https://doi.org:10.3389/fimmu.2020.00976

10 Biddison, W. E. *et al.* Chemokine and matrix metalloproteinase secretion by myelin proteolipid protein-specific CD8+ T cells: potential roles in inflammation. *J Immunol* **158**, 3046-3053 (1997).

11 Jin, L. *et al.* CXCR1- or CXCR2-modified CAR T cells co-opt IL-8 for maximal antitumor efficacy in solid tumors. *Nat Commun* **10**, 4016 (2019). https://doi.org:10.1038/s41467-019-11869-4

12 Vitanza, N. A. *et al.* Locoregional infusion of HER2-specific CAR T cells in children and young adults with recurrent or refractory CNS tumors: an interim analysis. *Nat Med* **27**, 1544-1552 (2021). https://doi.org:10.1038/s41591-021-01404-8

13 Loetscher, M. *et al.* Chemokine receptor specific for IP10 and mig: structure, function, and expression in activated T-lymphocytes. *J Exp Med* **184**, 963-969 (1996). https://doi.org:10.1084/jem.184.3.963

14 Ravanpay, A. C. *et al.* EGFR806-CAR T cells selectively target a tumor-restricted EGFR epitope in glioblastoma. *Oncotarget* **10**, 7080-7095 (2019). https://doi.org:10.18632/oncotarget.27389

15 Vitanza, N. A. *et al.* Locoregional CAR T cells for children with CNS tumors: Clinical procedure and catheter safety. *Neoplasia* **36**, 100870 (2023). https://doi.org:10.1016/j.neo.2022.100870

16 Vitanza, N. A. *et al.* Locoregional CAR T Cells for the Treatment of CNS Tumors in Children: Investigational Drug Service Pharmacy Activities. *J Hematol Oncol Pharm* **14**, 148-154 (2024).
17 Haydar, D. *et al.* Cell-surface antigen profiling of pediatric brain tumors: B7-H3 is consistently expressed and can be targeted via local or systemic CAR T-cell delivery. *Neuro Oncol* **23**, 999-1011 (2021). https://doi.org:10.1093/neuonc/noaa278
18 Majzner, R. G. *et al.* CAR T Cells Targeting B7-H3, a Pan-Cancer Antigen, Demonstrate Potent Preclinical Activity Against Pediatric Solid Tumors and Brain Tumors. *Clin Cancer Res* **25**, 2560-2574 (2019). https://doi.org:10.1158/1078-0432.CCR-18-0432
19 Biery, M. C. *et al.* A Protocol for the Generation of Treatment-naive Biopsy-derived Diffuse Intrinsic Pontine Glioma and Diffuse Midline Glioma Models. *J Exp Neurol* **1**, 158-167 (2020). https://doi.org:10.33696//Neurol.1.025
20 Reynders, N. *et al.* The Distinct Roles of CXCR3 Variants and Their Ligands in the Tumor Microenvironment. *Cells* **8** (2019). https://doi.org:10.3390/cells8060613
21 Korniejewska, A., McKnight, A. J., Johnson, Z., Watson, M. L. & Ward, S. G. Expression and agonist responsiveness of CXCR3 variants in human T lymphocytes. *Immunology* **132**, 503-515 (2011). https://doi.org:10.1111/j.1365-2567.2010.03384.x
22 Luster, A. D. & Ravetch, J. V. Biochemical characterization of a gamma interferon-inducible cytokine (IP-10). *J Exp Med* **166**, 1084-1097 (1987). https://doi.org:10.1084/jem.166.4.1084
23 Mount, C. W. *et al.* Potent antitumor efficacy of anti-GD2 CAR T cells in H3-K27M(+) diffuse midline gliomas. *Nat Med* **24**, 572-579 (2018). https://doi.org:10.1038/s41591-018-0006-x
24 Lin, G. L. *et al.* Non-inflammatory tumor microenvironment of diffuse intrinsic pontine glioma. *Acta Neuropathol Commun* **6**, 51 (2018). https://doi.org:10.1186/s40478-018-0553-x
25 Lieberman, N. A. P. *et al.* Characterization of the immune microenvironment of diffuse intrinsic pontine glioma: implications for development of immunotherapy. *Neuro Oncol* **21**, 83-94 (2019). https://doi.org:10.1093/neuonc/noy145
26 Wang, G. *et al.* CXCL11-armed oncolytic adenoviruses enhance CAR-T cell therapeutic efficacy and reprogram tumor microenvironment in glioblastoma. *Mol Ther* **31**, 134-153 (2023). https://doi.org:10.1016/j.ymthe.2022.08.021
27 Brown, C. E. *et al.* Optimization of IL13Ralpha2-Targeted Chimeric Antigen Receptor T Cells for Improved Anti-tumor Efficacy against Glioblastoma. *Mol Ther* **26**, 31-44 (2018). https://doi.org:10.1016/j.ymthe.2017.10.002
28 Theruvath, J. *et al.* Locoregionally administered B7-H3-targeted CAR T cells for treatment of atypical teratoid/rhabdoid tumors. *Nat Med* **26**, 712-719 (2020). https://doi.org:10.1038/s41591-020-0821-8
29 Donovan, L. K. *et al.* Locoregional delivery of CAR T cells to the cerebrospinal fluid for treatment of metastatic medulloblastoma and ependymoma. *Nat Med* **26**, 720-731 (2020). https://doi.org:10.1038/s41591-020-0827-2
30 Ghassemi, S. *et al.* Rapid manufacturing of non-activated potent CAR T cells. *Nat Biomed Eng* **6**, 118-128 (2022). https://doi.org:10.1038/s41551-021-00842-6

31 Mishra, H. K. & Kalyuzhny, A. Revolutionizing Cancer Treatments through Stem Cell-Derived CAR T Cells for Immunotherapy: Opening New Horizons for the Future of Oncology. *Cells* **13** (2024). https://doi.org:10.3390/cells13181516